Actuator control with H-infinity and mu-synthesis

Actuator control with $\mathcal{H}_\infty$-optimization and μ-synthesis

Marc van de Wal

WFW report 95.062

M.M.J. VAN DE WAL
Faculty of Mechanical Engineering
Eindhoven University of Technology
May 1995

Actuator control with $\mathcal{H}_\infty$-optimization and μ-synthesis

Marc van de Wal
Faculty of Mechanical Engineering
Eindhoven University of Technology

May 23, 1995

Trainee project
Supervisor: Bram de Jager

Summary

In this report, an attempt is made to design robust linear controllers for a rotary electro-mechanical actuator, which was proposed as a benchmark problem in [7]. For this purpose, controllers are designed based on the concepts of $\mathcal{H}_\infty$-optimization and μ-synthesis, the key ideas of which are briefly explained.

Meeting the tracking specifications in the presence of control input saturation, persistent load disturbance, and Coulomb friction appeared to be impossible. Only for the system without saturation, controller design was satisfactory.

The reason that the design is not successful is believed to be twofold. Firstly, incorporating nonlinearities such as saturation and Coulomb friction in the linear control system set-up is not always possible or straightforward, and might introduce conservativeness into the design. Secondly, controller design takes place in the frequency domain, while the specifications for the rotary actuator are formulated in the time domain. For this reason, frequency domain equivalents have to be found for the time domain requirements. Unfortunately, meeting the frequency domain specifications is not a guarantee for meeting the time domain specifications. As a consequence, designing controllers by $\mathcal{H}_\infty$-optimization and μ-synthesis largely becomes a trial-and-error procedure: modifications of the type and the parameters of weighting functions have to be evaluated by closed-loop responses repeatedly.

Contents

Chapter 1

Introduction

In modern control system design, *robust performance* is a major issue. This means that the controller must guarantee that the system remains stable *and* meets the performance objectives (*e.g.*, tracking, attenuation of disturbances and measurement noise), even in the presence of uncertainties (modeling errors). This property will be explained in more detail in Chapter 2.

Several robust control design methods can be employed, see, *e.g.*, [6]. Provided that the system model is linear and that the uncertainties are ∞-norm-bounded, robustly performing linear controllers can be designed by $\mathcal{H}_\infty$-optimization and μ-synthesis. The key ideas of these methods, which are the focus of this report, are outlined in Chapter 2 as well.

The benchmark problem proposed in [7], control of a rotary electro-mechanical actuator, will serve to illustrate both approaches for controller design. One characteristic of the system is "Coulomb friction" or "slip-stick friction" [5], which is a highly nonlinear phenomenon. As a consequence, special measures must be taken to account for friction in the necessarily linear control system set-up. A second nonlinearity in the system is due to saturation of the input signal. The system model, the model of the Coulomb friction, and the performance specifications are discussed in Chapter 3.

Controller design and closed-loop control system evaluation is considered in Chapter 4. Starting with a relatively simple, "peeled-off" control problem, additional design requirements are introduced step-by-step. However, it is emphasized that the goal of the study reported here is *not* to search for the ultimately performing controller for the particular system, but rather to illustrate the (im)possibilities of $\mathcal{H}_\infty$- and μ-based controller design methods, to compare both methods, and to illustrate some of the typical problems which may occur when designing controllers in this way.

Finally, the main findings with respect to $\mathcal{H}_\infty$- and μ-based controller design methods are listed in Chapter 5. More specific conclusions for the actuator design example are drawn as well.

Chapter 2

Key ideas of $\mathcal{H}_\infty$-optimization and μ-synthesis

In this chapter, the fundamentals of two robust controller design methods to be used for the actuator control problem will be discussed.

2.1 Standard control system set-up

The standard framework of an uncertain linear time invariant control system is shown in Fig. 2.1. Block G represents the generalized plant, which includes the system to be controlled (the "plant"), possibly extended with weighting functions reflecting performance specifications and weighting functions which characterize the amount of uncertainty. The controller is denoted K. Uncertainties (modeling errors) are represented by Δ_u. A *fictitious* perturbation block Δ_p is introduced to account for performance specifications. In the sequel of this report, it is assumed that Δ_u and Δ_p are stable and that by weighting functions they are scaled such that $\|\Delta_u\|_\infty \leq 1$ and $\|\Delta_p\|_\infty \leq 1$, with the ∞-norm of a Transfer Function Matrix (TFM) T defined as follows [8, Section 5.5.2]:

$$\|T\|_\infty := \sup_{\omega \in \mathbb{R}} \overline{\sigma}(T(\mathrm{j}\omega)). \tag{2.1}$$

The inputs to the generalized plant G are: the output p of the uncertainty block Δ_u, the exogenous input w^*, *e.g.*, disturbances, measurement noise and reference signals, and the input u generated by the controller. The outputs of the generalized plant are the following: the input q to the uncertainty block Δ_u, the control objectives z^*, formulated such that z^* is ideally zero, and the measurements y. So, the plant has an open-loop TFM G such that:

$$\begin{bmatrix} q \\ z^* \\ y \end{bmatrix} = \begin{bmatrix} z \\ y \end{bmatrix} = \begin{bmatrix} G_{11} & G_{12} \\ G_{21} & G_{22} \end{bmatrix} \begin{bmatrix} w \\ u \end{bmatrix} = G \begin{bmatrix} p \\ w^* \\ u \end{bmatrix}. \tag{2.2}$$

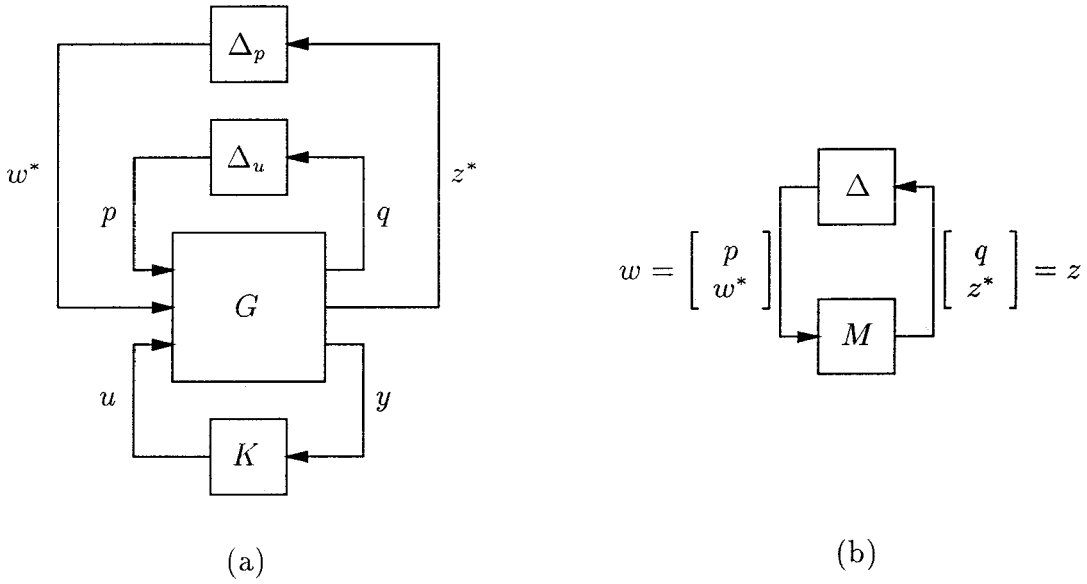

Figure 2.1: Standard control problem set-up

Figure 2.1(b) is obtained by closing the control loop in Fig. 2.1(a).The closed-loop TFM M can be written as a so-called lower Linear Fractional Transformation (LFT) of G and K:

$$\begin{aligned} M &= \mathcal{F}_l(G,K) := G_{11} + G_{12}K(I - G_{22}K)^{-1}G_{21}, \\ z &= \begin{bmatrix} q \\ z^* \end{bmatrix} = \begin{bmatrix} M_{11} & M_{12} \\ M_{21} & M_{22} \end{bmatrix} \begin{bmatrix} p \\ w^* \end{bmatrix} = Mw. \end{aligned} \tag{2.3}$$

The feedback system is said to be *well-posed* as long as $(I - G_{22}K)^{-1}$ is nonsingular [8, Section 6.3.3]. Furthermore, $\Delta = \text{diag}(\Delta_u, \Delta_p)$.

The *goal* of both $\mathcal{H}_\infty$-optimization and μ-synthesis is to find a controller $K(s)$ which, firstly, (robustly) *stabilizes* the closed-loop system, and, secondly *minimizes* the "norm" of the closed-loop TFM M from w to z, see Section 2.2 and 2.3. In order to design such a controller with the MATLAB "Robust Control Toolbox" [2] (abbreviated "RC-Toolbox") or with the "μ-Analysis and Synthesis Toolbox" [1] (abbreviated "μ-Toolbox"), a state-space representation of G is needed:

$$\begin{aligned} \dot{x} &= Ax + B_1 w + B_2 u \\ z &= C_1 x + D_{11} w + D_{12} u \\ y &= C_2 x + D_{21} w + D_{22} u, \end{aligned} \tag{2.4}$$

where x is the state of the system. Note that G must be proper for a state-space description to exist.

2.2 $\mathcal{H}_\infty$-Optimization

The control system in Fig. 2.1 is said to achieve *Robust Stability* (RS) if the system remains stable even in the presence of uncertainties Δ_u. A necessary and sufficient condition for RS under *all full* perturbations Δ_u with $\|\Delta_u\|_\infty \leq 1$ is, that M is nominally stable, and $\|M_{11}\|_\infty < 1$.

In analogy, a control system is said to achieve *Robust Performance* (RP) if the system remains stable *and* meets the performance specifications in the presence of uncertainties. Necessary and sufficient for RP is that M is robustly stable, *and* that the ∞-norm of the *perturbed* TFM from w^* to z^* in Fig. 2.1(a) is less than 1 for every Δ_u with $\|\Delta_u\|_\infty \leq 1$. This in turn, is equivalent to the condition that M is nominally stable, *and* that the *augmented* perturbation model of Fig. 2.1(a) is *stable* for every Δ_u and Δ_p, both with ∞-norm less than or equal to 1 [8, Section 5.8.2]. So, by introducing the fictitious perturbation Δ_p, the RP problem is translated into a RS problem. Note that when Δ_p is not present, the RP problem reduces to the original RS problem, while in the absence of Δ_u a *Nominal Performance* (NP) problem is considered. A thorough discussion on RS, NP, and RP can be found in [4].

A *necessary and sufficient* condition for RS of the system in Fig. 2.1(b) is the following: provided M is nominally stable, M is robustly stable for *all full* perturbation blocks Δ with $\|\Delta\|_\infty \leq 1$ *if and only* if $\|M\|_\infty < 1$. For the RP problem, Δ is restricted to the block-diagonal structure $\text{diag}(\Delta_u, \Delta_p)$, hence the following *sufficient* condition for RP can be formulated:

> Robust performance of the closed-loop system under *all* perturbations Δ with $\|\Delta_u\|_\infty \leq 1$ and $\|\Delta_p\|_\infty \leq 1$ is achieved *if*
>
> 1. the closed-loop system M is nominally stable, *and*
> 2. $\|M\|_\infty < 1$.

By explicitly accounting for the fact that the off-diagonal blocks in Δ are zero, a *necessary and sufficient* condition for RP can be formulated. This will be discussed in Section 2.3.

Since it can not be expected that it is always possible (or necessary) to design a controller K which stabilizes the *entire* closed-loop system, the requirement that K stabilizes M is now interpreted as the more limited requirement that it stabilizes the loop around G_{22}, *i.e.*, that it stabilizes the system in Fig. 2.2 [8, Section 6.3.2].

The goal of the *sub-optimal* $\mathcal{H}_\infty$ control problem is to design a stabilizing K which achieves $\|M\|_\infty < 1$, while the goal of $\mathcal{H}_\infty$ *optimal* control is to find a stabilizing K which *minimizes* $\|M\|_\infty$. Using one of the MATLAB toolboxes, numerical problems can be circumvented if a sub-optimal controller is designed instead of the optimal one [6, Section 4.2.1.3].

When the controller design is based on the state-space representation in (2.4), the following conditions must hold for the MATLAB algorithms to find a solution [8, Section 6.5.7]:

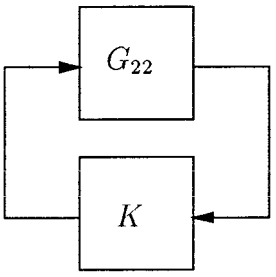

Figure 2.2: The loop around G_{22}

1. (A, B_2) is stabilizable and (C_2, A) is detectable.
   comment: This assumption ensures that the *whole* feedback system is stabilized, not just the loop around G_{22}.
2. D_{12} has full column rank, hence D_{12} is tall, and D_{21} has full row rank, hence D_{21} is wide.
3. $\begin{bmatrix} A - \mathrm{j}\omega I & B_2 \\ C_1 & D_{12} \end{bmatrix}$ has full column rank for all $\omega \in \mathbb{R}$.
4. $\begin{bmatrix} A - \mathrm{j}\omega I & B_1 \\ C_2 & D_{21} \end{bmatrix}$ has full row rank for all $\omega \in \mathbb{R}$.

The controller design requires solving two Riccati equations, the solutions of which define an observer *cum* state feedback law, see, *e.g.*, [8, Section 6.5.7]. A stabilizing controller K which achieves $\|M\|_\infty < 1$ for *all full* perturbation blocks Δ with $\|\Delta\|_\infty \leq 1$ exists, *if and only if* the solutions to the Riccati equations are positive semidefinite, the spectral radius of the product of the two solutions is less than 1, and, finally, if $\overline{\sigma}(D_{11}) < 1$ [2, Chapter 1]. In case Δ is not a full perturbation block, *e.g.*, if $\Delta = \mathrm{diag}(\Delta_u, \Delta_p)$, these conditions are not necessary anymore, but only *sufficient*.

Application of one of the before-mentioned MATLAB toolboxes will yield a proper controller. According to [8, Section 6.6], two types of solutions to the $\mathcal{H}_\infty$ problem of finding a K such that $\|M\|_\infty < \gamma$ are encountered:

1. *Type A solution.* The controller is stabilizing for all $\gamma \geq \gamma_0$, with γ_0 the lower bound of $\|M\|_\infty$, *i.e.*, $\|M\|_\infty \geq \gamma_0$. In this case, the *optimal* solution is obtained for $\gamma = \gamma_0$. Note that for the $\mathcal{H}_\infty$ control problem formulation in this report it is required that $\gamma \leq 1$.
2. *Type B solution.* The controller K is destabilizing for $\gamma < \gamma_{opt}$ with $\gamma_{opt} \geq \gamma_0$.

For the type B solution, the optimal controller is found for $\gamma = \gamma_{opt}$. A disconcerting phenomenon for this case is, that large coefficients occur in the state-space description of K. To avoid numerical problems, the optimum shouldn't be approached too closely.

In general, an $\mathcal{H}_\infty$ *sub-optimal* controller has the same order n as the augmented plant G in (2.4). An $\mathcal{H}_\infty$ *optimal* controller can be computed having at most $(n-1)$ states [2, Chapter 1]. A final important property of the optimal controller is, that the largest singular value $\overline{\sigma}(M(\mathrm{j}\omega))$ of the optimal closed-loop TFM M is *constant* as a function of the frequency ω. This is known as the "equalizing property" of optimal solutions [8, Section 6.6.1].

2.3 μ-Synthesis

In Section 2.2, a necessary and sufficient condition for RS of the control system in Fig. 2.1(b) was formulated: provided M is nominally stable, M is robustly stable for *all full* perturbation blocks Δ with $\|\Delta\|_\infty \leq 1$ if and only if $\|M\|_\infty < 1$. However, if $\|\Delta\|_\infty \leq 1$ is the only specification for Δ, this leaves the perturbation block completely *unstructured*, which may lead to an overly conservative controller design, in the sense that the amount of uncertainty accounted for is unnecessarily high. In the case of a RP problem, Δ is a *structured* perturbation block, since $\Delta = \mathrm{diag}(\Delta_u, \Delta_p)$. An $\mathcal{H}_\infty$ controller design as discussed in the previous section, does not take into account the zero off-diagonal blocks in Δ, but it assumes that perturbations may occur in these blocks as well. As a result, quite conservative estimates are obtained of the stability region for *structured* perturbations.

While in general the "performance block" Δ_p is unstructured, the uncertainty block Δ_u itself may be structured. So, not only the RP problem (with at least two unstructured blocks), but also the RS problem may ask for a controller design method based on a structured perturbation representation Δ. For this purpose, the concept of "structured singular value", commonly referred to as "μ", was proposed by Doyle [3]. In this approach, the overall perturbation Δ has the following block-diagonal form:

$$\Delta = \begin{bmatrix} \Delta_{u_1} & 0 & \cdots & \cdots & 0 \\ 0 & \Delta_{u_2} & & & \vdots \\ \vdots & & \ddots & & \vdots \\ \vdots & & & \Delta_{u_k} & 0 \\ 0 & \cdots & \cdots & 0 & \Delta_p \end{bmatrix}. \tag{2.5}$$

Given this perturbation model, $\mathcal{D}$ is defined as the class of constant complex-valued matrices of the same form as (2.5), with the diagonal blocks Δ_{u_i} of the following form:

- $\Delta_{u_i} = \delta I$, with δ a real number. If I has dimension 1 this represents a *real* scalar variation. Otherwise, it is a repeated real scalar perturbation.
- $\Delta_{u_i} = \delta I$, with δ a complex number. This represents a scalar, or repeated scalar, *dynamic* perturbation.
- Δ_{u_i} (and Δ_p), a complex-valued matrix. This represents a multivariable *dynamic* perturbation.

Unfortunately, the μ-Toolbox is restricted to structured *dynamic* perturbations. As a consequence, a real scalar perturbation must be represented by a scalar dynamic perturbation, potentially leading to a more conservative controller design. The RC-Toolbox does suggest a method to account for real parametric uncertainties, though the algorithm is not automated. However, this toolbox does not handle repeated perturbations.

The structured singular value $\mu_\Delta(T)$ of a complex-valued matrix T with respect to the perturbation structure in Δ is now defined as follows [1, Chapter 2]:

$$\mu_\Delta(T) := \frac{1}{\min\{\overline{\sigma}(\Delta):\ \Delta \in \mathcal{D},\ \det(I - T\Delta) = 0\}}, \tag{2.6}$$

unless no $\Delta \in \mathcal{D}$ makes $(I - T\Delta)$ singular, in which case $\mu_\Delta(T) = 0$.

So, the structured singular value $\mu_\Delta(T)$ is the inverse of the largest singular value of the smallest perturbation Δ within $\mathcal{D}$ that makes $(I - T\Delta)$ singular. Thus, the larger $\mu_\Delta(T)$, the smaller the perturbation Δ which is needed to make $(I - T\Delta)$ singular. In case of an unstructured Δ block, $\mu_\Delta(T) = \overline{\sigma}(T)$. For more details on the structured singular value, the reader is referred to [8, Section 5.7].

The use of the structured singular value for robustness analysis and robust controller design will be explained below. For this purpose, the μ-value for a TFM T is defined as the maximum value of μ over all frequencies [6, Section 4.2.2] (compare with (2.1)):

$$\|T\|_\Delta := \sup_{\omega \in \mathbb{R}} \mu_\Delta(T(\mathrm{j}\omega)). \tag{2.7}$$

In fact, $\|T\|_\Delta$ is not a norm, since it does not satisfy the so-called triangle inequality, see, *e.g.*, [8, Section 5.4.2].

A *necessary and sufficient* condition for RP of the control system in Fig. 2.1(b) is derived in [8, Section 5.7.3]:

> Robust performance of the closed-loop system under *all* structured perturbations $\Delta \in \mathcal{D}$ satisfying $\|\Delta\|_\infty \leq 1$ is achieved *if and only if*:
>
> 1. the closed-loop system M is nominally stable, *and*
> 2. $\|M\|_\Delta < 1$.

The goal of μ-synthesis is now to design a controller K which stabilizes the nominal feedback system and makes $\|M\|_\Delta < 1$, or minimizes $\|M\|_\Delta$ with respect to all stabilizing K's. Note that Δ in Fig. 2.1 represents knowledge of the structure and ∞-norm of Δ; additional information on Δ must be incorporated in G by means of weighting functions.

Unfortunately, exact μ-synthesis and -analysis are currently unsolved due to computational difficulties with $\mu_\Delta(M)$ for 3 or more uncertainty blocks [1, Chapter 2]. Instead, an approximate solution to the μ-synthesis problem is used. The approach used in the MATLAB

toolboxes will be referred to as D-K iteration. This approach relies on the property [8, Section 5.7.4]:

$$\mu_\Delta(M) \leq \overline{\sigma}(DM\overline{D}^{-1}), \tag{2.8}$$

with D and $\overline{D}$ diagonal scaling matrices. Suppose that the i-th diagonal block of Δ has dimension $m_i \times n_i$, then the i-th diagonal blocks of D and $\overline{D}$ are given by:

$$D_i = d_i I_{n_i}, \quad \overline{D}_i = d_i I_{m_i}, \tag{2.9}$$

with d_i a positive real number. If *repeated* perturbations are considered as well, the scaling matrices should take a different form, see, *e.g.*, [1, Chapter 2]. In this report, repeated perturbations do not play a role.

The problem of minimizing $\|M\|_\Delta$ is now replaced by minimizing the upper bound $\|DM\overline{D}^{-1}\|_\infty$, where for each frequency ω the matrices $D(\mathrm{j}\omega)$ and $\overline{D}(\mathrm{j}\omega)$ are chosen such that the bound is tightest possible. Minimizing $\|DM\overline{D}^{-1}\|_\infty$ with respect to K is a standard $\mathcal{H}_\infty$ problem, provided D and $\overline{D}$ are rational stable matrix functions.

The D-K iteration, see, *e.g.*, [8, Section 6.9.3.1], is now performed as follows:

1. Choose an initial controller that stabilizes the closed-loop system (*e.g.*, by an $\mathcal{H}_\infty$ controller design for an unstructured Δ block), and compute the corresponding nominal closed-loop TFM M.

2. Evaluate the upper bound

$$\min_{D(\mathrm{j}\omega),\, \overline{D}(\mathrm{j}\omega)} \overline{\sigma}(D(\mathrm{j}\omega)M(\mathrm{j}\omega)\overline{D}^{-1}(\mathrm{j}\omega)), \tag{2.10}$$

   with D and $\overline{D}$ diagonal matrices over a suitable frequency grid. The maximum of this upper bound over the frequency grid is an estimate of $\|M\|_\Delta$. If $\|M\|_\Delta$ is "small enough" (depends on specified tolerance), stop, otherwise, continue.

3. On the frequency grid, fit stable minimum phase rational functions to the diagonal entries d_i of D and $\overline{D}$, and replace the original data in D and $\overline{D}$ with their rational approximations. The fit is only in magnitude, and the freedom in the phase allows the rational functions to be defined as stable and minimum phase.

4. Given D and $\overline{D}$, minimize $\|DM\overline{D}^{-1}\|_\infty$ with respect to all stabilizing controllers. Denote the minimizing controller as K and the corresponding closed-loop TFM as M, and return to step 2.

So, the D-K iteration is in fact an intertwined $\mathcal{H}_\infty$-controller design and μ-analysis sequence. The D-K iteration continues until the μ-value doesn't change significantly anymore between two iterations. Convergence of this algorithm is *not* always guaranteed. Moreover, the combined D-K iteration procedure is not convex, so in general the resulting μ-synthesis controller is sub-optimal. The *controller* order is in general equal to the order n of the generalized plant $G(s)$ plus twice the order of $D(s)$ [2, Chapter 2]. Since the controller order must often be restricted due to implementation limits (see, *e.g.*, [10]), it may be advisable to use low order scalings. Another option is to apply order reduction to the computed controller.

Chapter 3

Actuator control problem

The system to be controlled and the performance specifications, obtained from [7], will be described in Section 3.1. In Section 3.2, one way to model the Coulomb friction as proposed in [5] will be discussed.

3.1 System description and performance specifications

The use of electro-mechanical actuators is widely spread, *e.g.*, in robots for car manufacturing. A block diagram of the *model* of the rotary electro-mechanical actuator to be considered is presented in Fig. 3.1. In this figure, the signals have the following meaning:

- u commanded input,
- x_1 position,
- x_2 angular velocity,
- M_l persistent load disturbance.

The model employs the following simplifications. It

- neglects the dynamics of the electrical motor,
- ignores the load dynamics, and it
- neglects viscous friction.

The Coulomb friction model accounts for both "slip" and "stick", see Section 3.2. The model parameters are partially uncertain and are presented in Table 3.1.

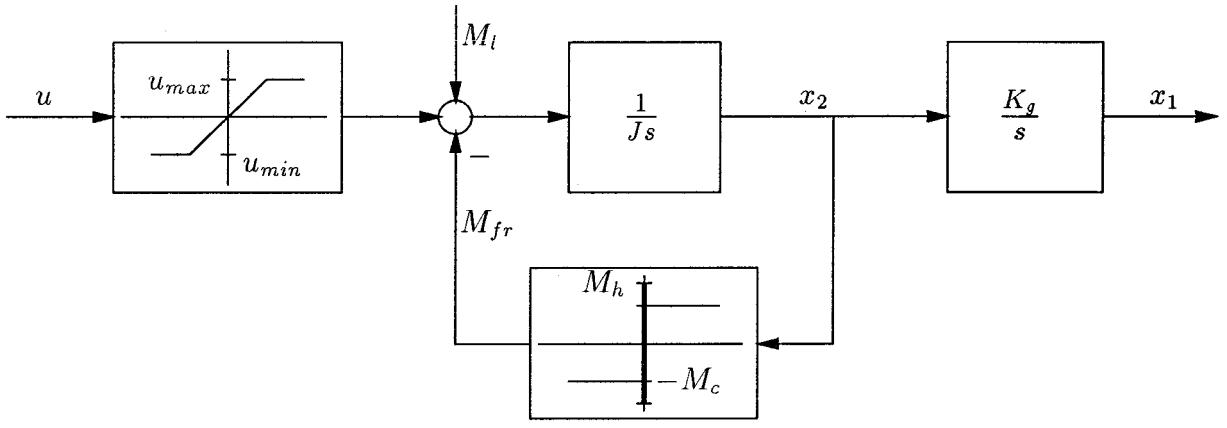

Figure 3.1: Model of a rotary electro-mechanical actuator

Parameter	Symbol	Value	Unit
moment of inertia	J	400	[kg mm^2]
conversion factor	K_g	7.04	[mm/2πrad]
static load	M_l	1.5	[Nm]
Coulomb friction (slip)	M_c	0.3...0.8	[Nm]
Coulomb friction (stick)	M_h	$2M_c \leq M_h \leq 3M_c$	[Nm]
maximal input	u_{max}	4.0	[Nm]
minimal input	u_{min}	-4.0	[Nm]
maximal position range	$x_{1,max}$	$\pm$ 15	[mm]

Table 3.1: Model parameters

The main task of the system is to make x_1 follow a desired step-wise change in position of 3.5 [mm]. For this task, the specifications are as follows:

1. the settling time T_{98} must be less then 50 [ms], *i.e.*, within 50 [ms] x_1 must reach and remain within 2 percent of the step size,
2. the final position accuracy must be better than 0.04 [mm],
3. overshoot is not permitted.

Furthermore, the system should also fulfill the first two requirements for step-wise changes in the required position of small magnitude, *e.g.*, 0.1 [mm], and of large magnitude, *e.g.*, from -7.5 [mm] to 7.5 [mm] [7].

The time between two step-wise changes of the desired position is at least 60 [ms].

The controller must be implemented as a digital one with a sampling frequency of no more than 2 [kHz]. The only measurement is the position, available with an accuracy of 12 binary digits, related to the maximal range $x_{1,max}$.

Comments:

The following illustrates that fulfilling the requirements for step-wise changes from -7.5 [mm] to 7.5 [mm] is impossible. If, from standstill, the maximum input u_{max} is applied to the system without friction and static load, the maximum displacement within T_{98} [s] equals $\frac{K_g}{2J} u_{max}(T_{98})^2 \approx 14$ [mm]. For this reason, a different specification will be used: the system should fulfill the first two requirements for step-wise changes from -6 [mm] to 6 [mm].

However, it remains questionable if the specifications for large step-wise changes can be met, as will be shown next. The fastest way to move x_1 from 0 to w^* within T_{98} *without* overshoot, is to accelerate with full force in the first part of the traject, and to decelerate using full force in the second part. Suppose $M_{fr} = M_c \text{sign}(x_2)$, $M_c = 0.8$ and $w^* > 0$. A simple calculation shows that w^* is now maximally 6.8 [mm]. In case $w^* < 0$, $|w^*|$ is maximally 4.7 [mm]. For this reason, it is expected that meeting the requirements for step-wise changes larger than 4.7 [mm] is very hard, even though overshoot is allowed for large step-wise changes.

3.2 Coulomb friction model

Friction is often responsible for many problems associated with the control and accuracy of mechanical systems. For example, it may cause large tracking errors, and limit cycling around a final position. As a consequence, in Chapter 4 it is attempted to take friction into account during controller design.

Generally, Coulomb friction is represented as a nonlinear function of the relative velocity of two bodies in contact. The Coulomb friction force (or Moment) M_{fr} acts opposite to the

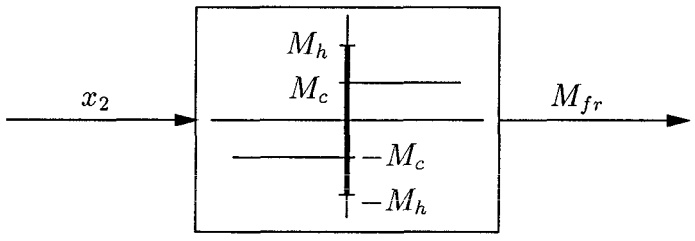

Figure 3.2: Coulomb friction model

direction of the relative velocity x_2, see Fig. 3.2, which is a part of Fig. 3.1. Two cases must be distinguished:

1. The relative velocity x_2 of the bodies is zero. This will be referred to as the "sticking" phase of friction. If a force is applied on a body *at rest*, it will not move until the applied force exceeds the peak stiction force M_h. For the electro-mechanical actuator $2M_c \leq M_h \leq 3M_c$, with M_h the constant Coulomb friction moment in motion ($x_2 \neq 0$). In [5], it is made plausible, that in sticking mode the friction is best described by a position-dependent relation.

2. The relative velocity x_2 of the bodies is *not* equal to zero. This will be referred to as the "slipping" phase of friction. When a body is moving at a certain velocity, a force M_c will act on it, in the opposite direction of x_2. Especially at low speeds, the magnitude of this force depends on x_2. However, to simplify the Coulomb friction model, M_c will be chosen constant as in Fig. 3.2.

In [5], a Coulomb friction model is proposed which is stated to be well-suited for simulation purposes. It is stated that it is numerically efficient, nevertheless retaining the essential features of Coulomb friction. The model is easy to implement (as will be shown) and only needs x_2 as the input (as in Fig. 3.2). An auxiliary integrator is used to represent stiction. Since the input to the integrator is turned off under certain conditions, the Coulomb friction model is called "reset integrator". It is described as follows:

if ($x_2 > 0$ and $p \geq p_0$) or ($x_2 < 0$ and$p \leq -p_0$)
$\dot{p} = 0$ (slip)
else
$\dot{p} = x_2$ (stick)
end
if $|p| < p_0$
$M_{fr} = \lambda(1 + \psi)p + \beta\dot{p}$ (stick)
else
$M_{fr} = \lambda p$ (slip)
end

Here, p is the position variable which is internally generated (state variable) by the Coulomb friction model. Note that the sticking friction is represented as a function of bot the position p and the velocity $\dot{p}$. As soon as $|p|$ reaches p_0 the system enters into slipping mode and $\dot{p} = 0$. An S-function block in SIMULINK is used to represent the friction model.

In the Coulomb friction model various parameters play a role, the use of which is explained below:

- p_0: This parameter defines the maximum amount of motion during sticking. It seems best to make p_0 small relative to the smallest positional increment of interest, which is $2\pi \cdot 0.04/K_g$ [rad] for the actuator considered here. For instance, p_0 might be set to 10% of this value.
- λ: This constant determines the amount of slip friction. If $\lambda = M_c/p_0$, the amount of friction M_{fr} during slip equals M_c.
- ψ: Generally, the maximum stick friction M_h is larger than the amount of friction in slip mode M_c. Parameter ψ is used to account for this. Suppose $M_h = \alpha M_c$, then ψ must be set $\alpha - 1$.
- β: A damping term $\beta\dot{p}$ is introduced to eliminate undamped oscillations *only* when in sticking mode. These oscillations would occur if the model is used in a system with no other damping. In the absence of any information characterizing this damping, β can be set to $\frac{1}{2}\sqrt{2}$ [5]. However, by simulations it is observed that if $\beta \neq 0$, the maximum stick friction may be substantially larger than specified by ψ. For this reason, β will fixed at zero for simulations with the electro-mechanical actuator.

In Fig. 3.3, the influence of Coulomb friction for the actuator system in Fig. 3.1 is illustrated for $M_l = 0$ and u a sinusoid with amplitude 4 [Nm] and frequency $1/T_{98}$ [Hz]. From the left figure, it is concluded that for $t < 10$ [ms], when the system is in sticking mode, M_{fr} approximately cancels u. Once $|p| > p_0$, M_{fr} drops back to M_c, the inertia J begins to slide and $x_2 \not\approx 0$ anymore, see right figure. The effect of $\beta = 0$ is also clearly visible. For more details on the friction model, the reader is referred to [5].

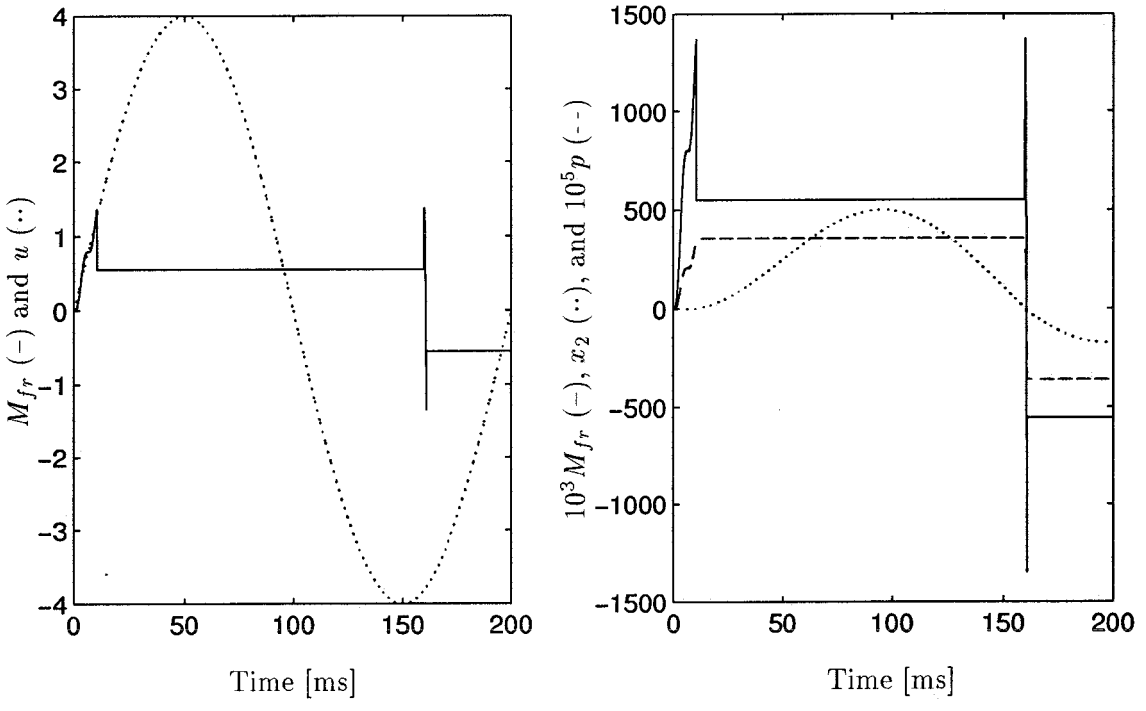

Figure 3.3: Effect of stick-slip friction: $p_0 = 0.1 \cdot 2\pi \cdot 0.04/K_g$, $\lambda = 0.55/p_0$, $\psi = 1.5$, $\beta = 0$

Chapter 4

Controller design and evaluation

In this chapter, $\mathcal{H}_\infty$- and μ-based controllers will be designed for the electro-mechanical actuator. The control problem will be augmented step-by-step. First, a *continuous* controller with one input y will be designed and evaluated for the system *without* Coulomb friction M_{fr}, *without* load M_l, and *without* saturation (Section 4.1). Secondly, control input saturation will be addressed in the controller design and incorporated in the simulation model (Section 4.2), followed by design and evaluation for the constant load and Coulomb friction, but in the *absence* of saturation (Section 4.3). Finally, Section 4.4 is devoted to the design and evaluation of controllers with 2 and 3 inputs y respectively, for the complete problem.

4.1 Design and evaluation for nominal tracking

To gain insight in the controller design methods of Chapter 2, the simplified problem in Fig. 4.1 will be studied first. Comparing this figure with Fig. 2.1, it is concluded that $q = 0, p = 0$ (so, $\Delta_u = 0$) and that:

$$G = \begin{bmatrix} W_y & -W_y P \\ 1 & -P \end{bmatrix}, \quad M = W_y(1 - PK(1+PK)^{-1}) = W_y(1-T) = W_y S, \tag{4.1}$$

with $S = (1+PK)^{-1}$ the so-called *sensitivity* function, and $T = PK(1+PK)^{-1}$ the *complementary sensitivity* function. Obviously, this is a *Nominal Performance* (NP) control problem aiming at minimizing $\|M\|_\infty$, which is the ∞-norm of the closed-loop transfer function between the reference signal w^* and the *weighted* tracking error z^*. Note that for this case $\Delta = \Delta_p$, which is a one-dimensional block without structure. So, μ-synthesis and $\mathcal{H}_\infty$-optimization come down to the same problem. Satisfactory performance is said to be obtained if $|S| < |S_{spec}| = |W_y^{-1}|$, or, equivalently, if $\|M\|_\infty < 1$.

In order to achieve the time-domain specifications formulated in Section 3.1 (settling time, no overshoot *etc.*), S_{spec} must be chosen suitably. So as to limit the order of G, and therefore

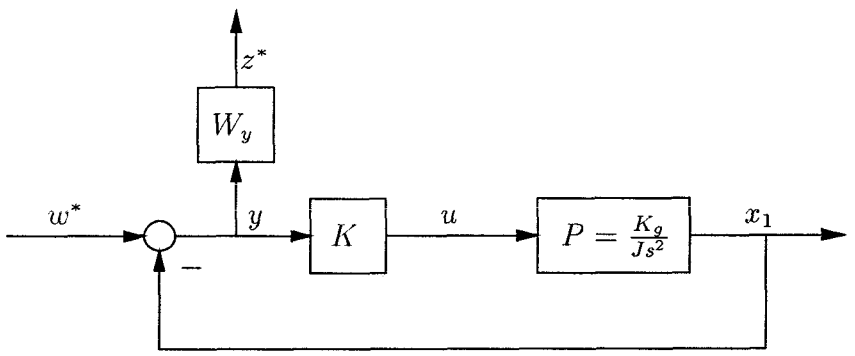

Figure 4.1: Control system including weighting function for tracking error

First setting		Second setting
$S_{spec,1}$	$S_{spec,2}$	$S_{spec,1}$
$\kappa = 1$	$\kappa = 1$	$\kappa = 2$
$a = 100$	$a_1 = 100$	$a = 100$
	$a_2 = (0.04 \cdot a_1)/(12 \cdot \kappa)$	

Table 4.1: Parameters for sensitivity specifications

the controller order, S_{spec}'s of order 1 will be used, for example:

$$S_{spec,1} = \kappa \frac{s}{s+a}, \quad S_{spec,2} = \kappa \frac{s+a_2}{s+a_1}. \tag{4.2}$$

The parameters of $S_{spec,1}$ and $S_{spec,2}$ are listed in Table 4.1. In both cases, κ is fixed at 1. For $S_{spec,1}$ the settling time specification is met, without overshoot, if $a \geq -\ln(0.02/\kappa)/T_{98} \approx 78$. Note that $S_{spec,1}(0) = 0$, specifying that steady-state errors are not allowed. Less demanding specifications for S, at least for low frequencies, might be imposed by using $S_{spec,2}$: a_1 is set to meet the settling time specification, *e.g.*, $a_1 = 100$, while a_2 is set to obtain a final accuracy of x_1 better then 0.04 [mm] for the "worst case" situation that a step-wise change of 12 [mm] occurs: $a_2 = (0.04 \cdot a_1)/(12 \cdot \kappa)$.

A straightforward design of an $\mathcal{H}_\infty$ controller for the system in Fig. 4.1 is not possible, since the second and fourth standard assumption in Section 2.2 are not satisfied: $D_{12} = 0$, so it does not have full column rank, and the plant $G(s)$ has at least two poles at $s = 0$, so the fourth assumption is not satisfied at $\omega = 0$.

To resolve the first problem, a very small weight on u is imposed: $W_u = 10^{-8}$, yielding $D_{12} = [0\ 10^{-8}]^T$. The second problem is solved by using a special type of "bilinear transformation", see, *e.g.*, [2, Chapter 1]. The eigenvalues of $A - \mathrm{j}\omega I$ on the imaginary axis are shifted to the $(-\alpha + \mathrm{j}\omega)$-axis by modifying A to $A - \alpha I$. The positive real number α must be chosen so the behavior of the plant is not significantly changed in the frequency range of interest, *i.e.*, in the frequency range between 0.01 and 1000 [rad/s]. If $\alpha = 10^{-6}$, the singular values of the original plant and of the modified plant are "the same" in this frequency range. With these modifications, an $\mathcal{H}_\infty$ controller can be designed. After the computation, the system matrix

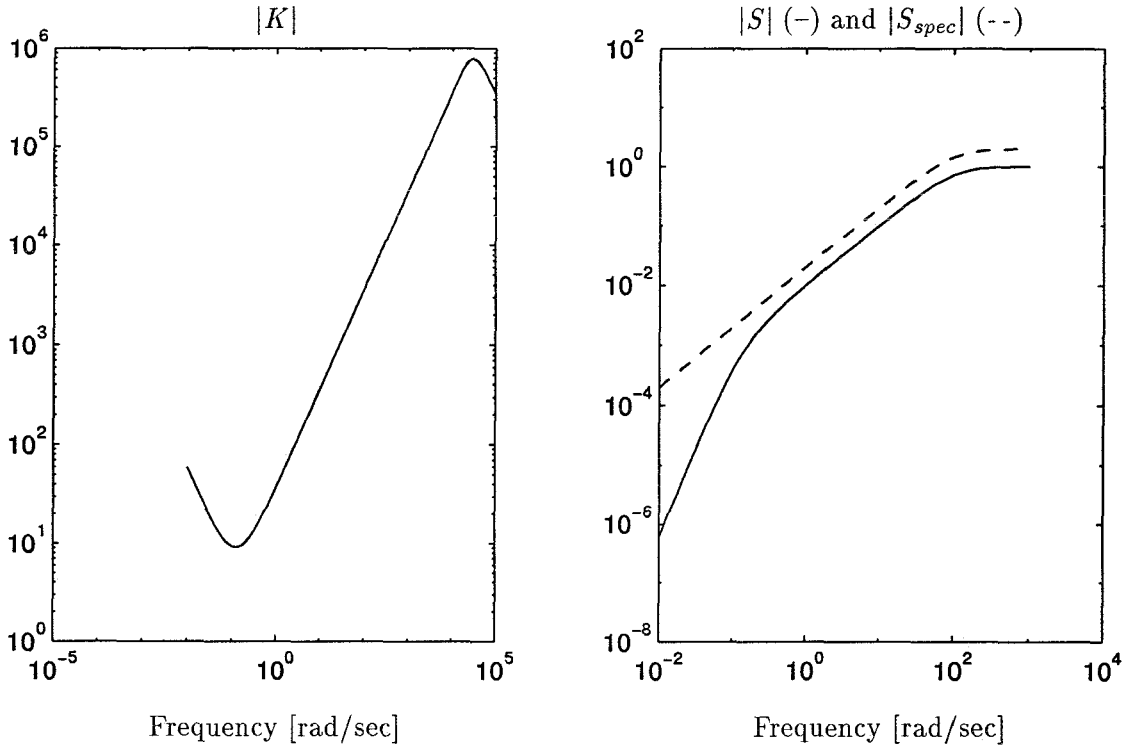

Figure 4.2: *left plot:* magnitude of the controller in (4.3); *right plot:* sensitivity and specified sensitivity

A_K of the controller K must be transformed back to $A_K + \alpha I$. The resulting controller is a sub-optimal solution to the original $\mathcal{H}_\infty$ control problem.

In both this section and the following ones, controller design is aimed at *minimizing* γ such that either $\|M\|_\infty < \gamma$ ($\mathcal{H}_\infty$-optimization), or $\|M\|_\Delta < \gamma$ (μ-synthesis). For the specified goal to be achieved, *e.g.*, NP, RS, or RP, γ must be 1 or smaller. With $S_{spec,1}$ and $S_{spec,2}$ according to the first setting in Table 4.1, controllers are computed for which γ is slightly larger than 1, *i.e.*, NP is not guaranteed.

If κ is raised, the requirements on S become less severe, and NP is easier achieved. For instance, if $\kappa = 2$, retaining the same settings for a, a_1, and a_2, the designed controllers make $\overline{\sigma}(M)$ flat in the frequency range of interest and achieves $\gamma = 0.51$. Note that these S_{spec}'s still represent the time domain specifications of interest. With $S_{spec,1}$, the following strictly proper controller is computed with the μ-Toolbox:

$$K(s) = \frac{3.40 \cdot 10^{10} s^2 + 1.01 \cdot 10^3 s - 5.66 \cdot 10^8}{s^3 + 4.39 \cdot 10^4 s^2 + 9.57 \cdot 10^8 s - 1.84 \cdot 10^{-5}}. \tag{4.3}$$

The left plot of Fig. 4.2 shows the magnitude of this controller. Obviously, the coefficients in the numerator and denominator polynomials are very large, which indicates that the solution is of type B, see Section 2.2. However, fixing "`tol`" at 0.1 instead of 0.01 [1, `hinfsyn`], in this way trying to prevent approaching the optimal solution too close, the controller coefficients remain large. On the other hand, if `tol` is set smaller than 0.01, the coefficients become even

larger than in (4.3). In the right plot of Fig. 4.2 it is shown that the sensitivity specification is met with controller (4.3).

In Fig. 4.3, results for a closed-loop simulation for the system in Fig. 4.1 are displayed. The desired trajectory w^* is chosen so all step-wise changes of interest are incorporated, by which all time domain specifications in Section 3.1 can be checked. During the simulation, w^* takes 4 different values other than zero: w^*=3.5 [mm] (I), w^*=−6 [mm] (II), w^*=6 [mm] (III), and w^*=0.1 [mm] (IV). The time between two step-wise changes in w^* is always 60 [ms]. Within the settling time, x_1 must be and remain within 2% of the step size of interest. The corresponding "target zone" for the tracking error y is indicated by the dashed line in the lower plot of Fig. 4.3 ($0.02 \cdot \delta w^*$). The times at which x_1 must be and remain inside this zone are indicated by a "*".

For this controller design, NP is achieved: overshoot does not occur, the settling time specifications are met (see Fig. 4.3, lower plot), and the final position error y is smaller than 0.04 [mm]. In fact, y asymptotically approaches zero, because $S(0) = 0$.

It is emphasized that large control inputs u are required during this simulation. At the time instants that w^* changes, peak values of u with an order of magnitude of 10^3 [Nm] occur. A simulation shows that if the system input saturates for controller outputs u larger than 4 [Nm], the performance specifications are not achieved with the proposed controller (4.3). For this reason, the next section is devoted to controller design taking saturation into account.

4.2 Design and evaluation for saturation

In this section, controller design and evaluation will be performed for the system with controller output saturation. Two distinct ways to account for saturation will be studied. In the first approach (Section 4.2.1), u is simply weighted, *i.e.*, a weighted version of the controller output u is added to z^*. In the second approach (Section 4.2.2), the nonlinear saturation element is modeled as a sector bounded uncertainty, see, *e.g.*, [2, Chapter 1] and [8, Section 5.5.5]. The latter approach makes the Δ block structured, by which μ-synthesis becomes worthwhile.

4.2.1 Weighting the controller output

Consider Fig. 4.4, in which the weighted input z_2^* is an additional control objective. Comparing this figure with Fig. 2.1, it is concluded that $q = p = 0$ ($\Delta_u = 0$), $z^* = [z_1^*\ z_2^*]^T$, and that:

$$G = \begin{bmatrix} W_y & -W_y P \\ 0 & W_u \\ 1 & -P \end{bmatrix}, \quad M = \begin{bmatrix} W_y S \\ W_u R \end{bmatrix}, \tag{4.4}$$

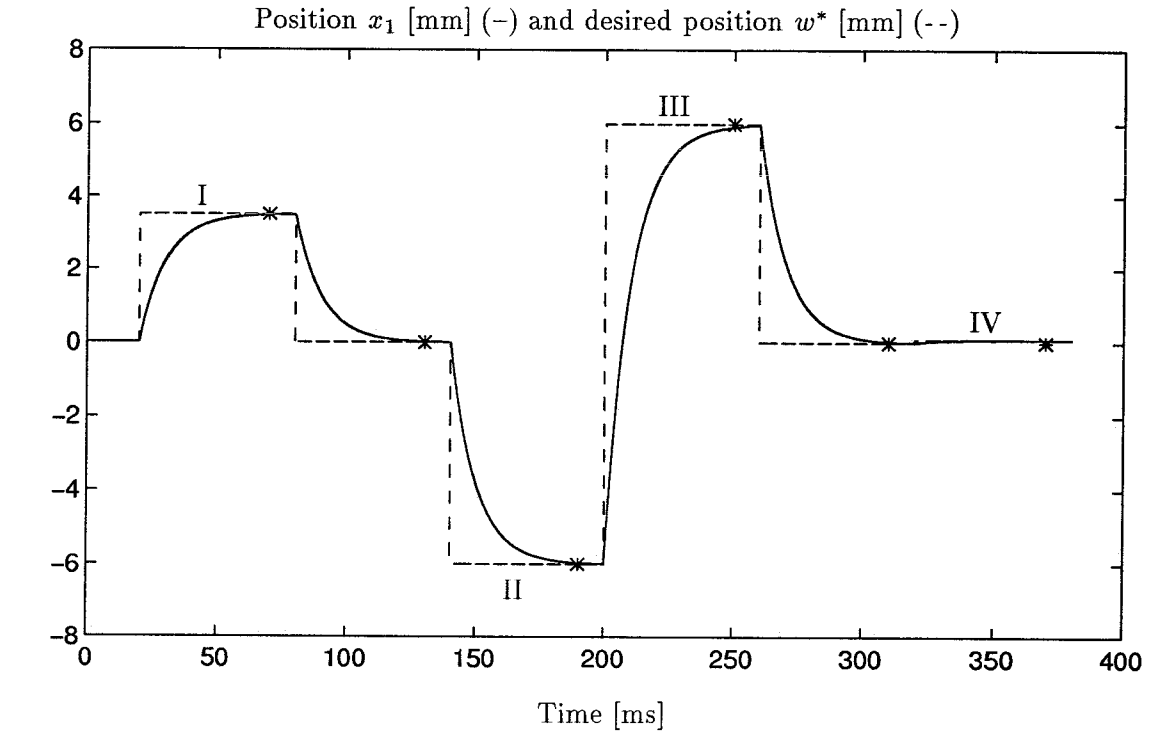

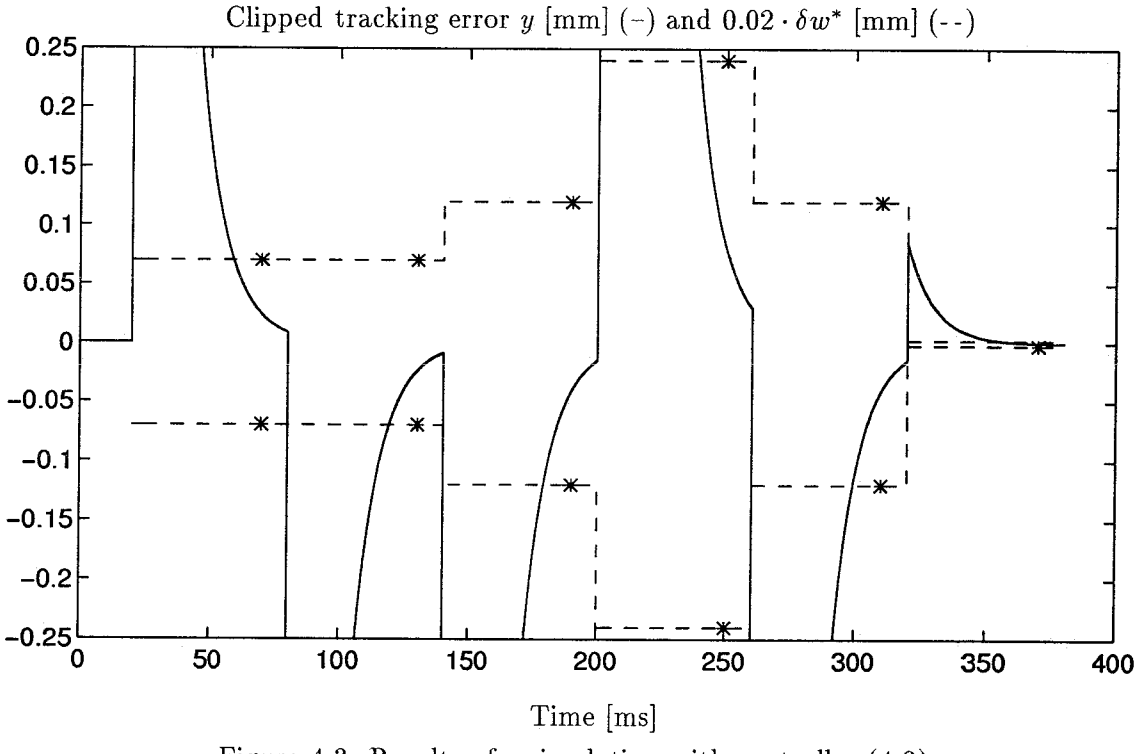

Figure 4.3: Results of a simulation with controller (4.3)

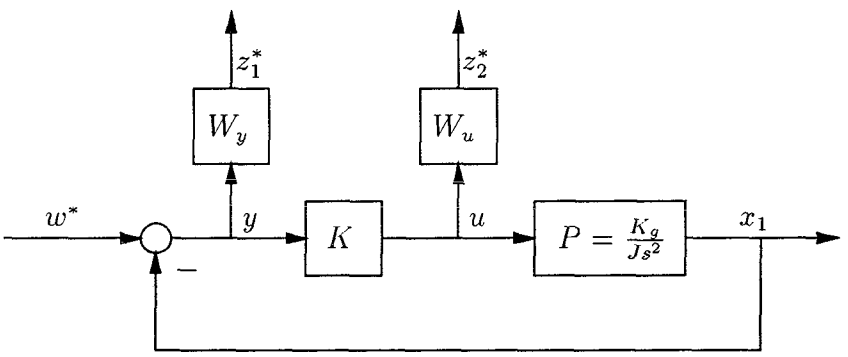

Figure 4.4: Control system including weights on tracking error y and control input u

with $R = K(1 + PK)^{-1}$ the so-called *input sensitivity* function. Again, this is a NP control problem with Δ_p a 1×2 unstructured block. For the SISO S and R considered here, minimizing $\|M\|_\infty$ comes down to minimizing [8, Section 6.2]:

$$\sup_{\omega \in \mathbb{R}} (|W_y(j\omega)S(j\omega)|^2 + |W_u(j\omega)R(j\omega)|^2) \tag{4.5}$$

with respect to all stabilizing controllers K. The solution often has the equalizing property, *i.e.*, the frequency-dependent function whose peak value is minimized is a constant γ (which must be smaller than 1 for the control problems in this report):

$$|W_y(j\omega)S(j\omega)|^2 + |W_u(j\omega)R(j\omega)|^2 = \gamma^2. \tag{4.6}$$

So, for the optimal solution:

$$|S(j\omega)| \leq \frac{\gamma}{|W_y(j\omega)|} \quad \omega \in \mathbb{R}, \tag{4.7}$$

$$|R(j\omega)| \leq \frac{\gamma}{|W_u(j\omega)|} \quad \omega \in \mathbb{R}. \tag{4.8}$$

By choosing the weighting functions W_y and W_u correctly, the functions S and R may be made small in appropriate frequency regions.

Performance is said to be satisfactory if $|S| < |S_{spec}| = |W_y^{-1}|$ *and* if $|R| < |R_{spec}| = |W_u^{-1}|$. The sensitivity will be specified by $S_{spec,1}$ in (4.2). To start with, the parameters of the second setting of $S_{spec,1}$ will be used, see Table 4.1. In order to avoid high frequency components in u, which occur for step-wise changes in w^* and cause saturation of u, high frequencies in u must be penalized. This is accounted for by the following choice of R_{spec}:

$$R_{spec} = \zeta \frac{s + b}{s}. \tag{4.9}$$

As it will appear (Fig. 4.7), $|W_y(j\omega)S(j\omega)|$ dominates at low frequencies, where W_y is large, while $|W_u(j\omega)R(j\omega)|$ dominates at high frequencies, where W_u is large.

The parameters ζ and b in R_{spec} must be chosen so the time domain specifications are achieved under control input saturation. Parameter b is used to indicate the frequency above which u

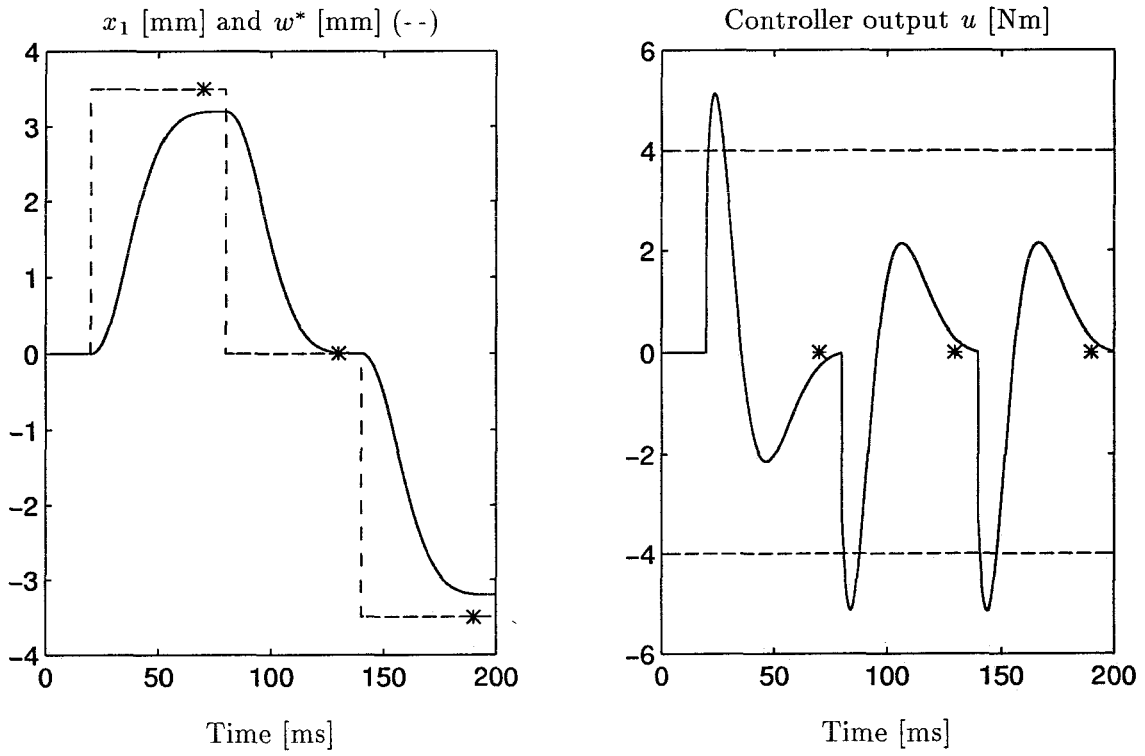

Figure 4.5: Closed-loop response for the main task $w^* = \pm 3.5$ [mm]

First setting		Second setting	
$S_{spec,1}$	R_{spec}	$S_{spec,1}$	R_{spec}
$\kappa = 2$	$\zeta = 1100$	$\kappa = 3$	$\zeta = 1100$
$a = 100$	$b = 2\pi/(10 \cdot 10^{-3})$	$a = 100$	$b = 2\pi/(10 \cdot 10^{-3})$

Table 4.2: Parameters for inverse weighting functions

must be penalized. Because of the settling time requirement ($T_{98} = 50$ [ms]), control signals of 20 [Hz] must be allowed. It seems reasonable to fix b at $2\pi/(10 \cdot 10^{-3})$ [rad/s], *i.e.*, frequencies in u above 100 [Hz] are penalized most severely. Unfortunately, finding a good setting for ζ is not straightforward, but based on a trial and error procedure.

Computing an $\mathcal{H}_\infty$ controller with $\zeta = 1$ yields $\gamma = 4.97$, so NP is *not* guaranteed. This γ can be reduced by increasing ζ, which implies that, compared with S, less demanding specifications are imposed on R over the whole frequency range. For $\zeta > 1000$, γ's are found which are smaller than 1. For the first setting in Table 4.2, $\gamma = 0.98$. However, a closed-loop simulation shows, that although the frequency domain specifications are met, the *time domain* specifications are *not*, see Fig. 4.5. This illustrates, that due to the limited possibility to translate time domain specifications into equivalent frequency domain specifications, an $\mathcal{H}_\infty$ controller design is not always solved straightforwardly.

It is now attempted to get a better performance by iteratively changing parameters in $S_{spec,1}$ and R_{spec}. For $\kappa = 3$ instead of $\kappa = 2$ (second setting in Table 4.2), $\gamma = 0.71$ is achieved for

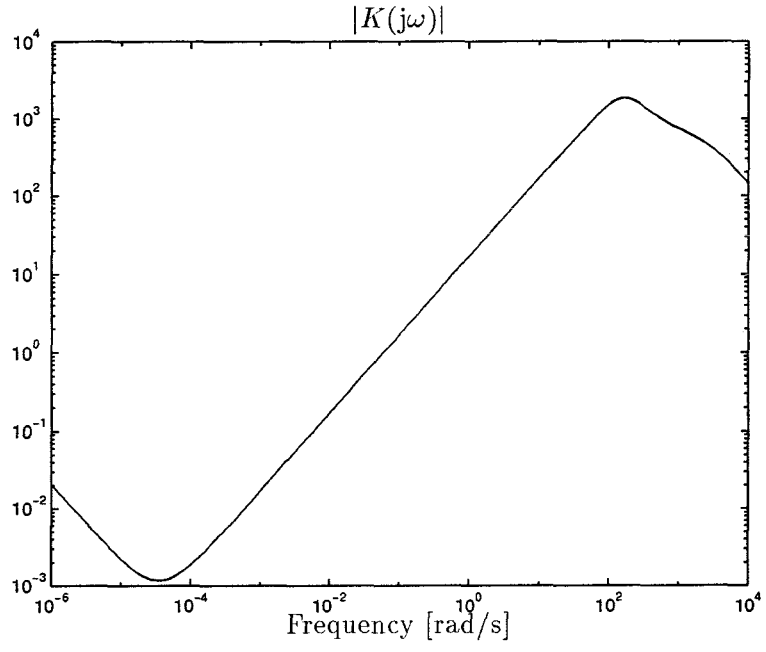

Figure 4.6: Magnitude plot of controller (4.10)

the following fourth order controller that is obtained with the μ-Toolbox:

$$K(s) = \frac{1.49 \cdot 10^6 s^3 + 9.37 \cdot 10^8 s^2 - 9.80 \cdot 10^{-3} s - 1.15}{s^4 + 2.39 \cdot 10^3 s^3 + 5.48 \cdot 10^5 s^2 + 5.61 \cdot 10^7 s - 5.08 \cdot 10^{-7}}. \tag{4.10}$$

The magnitude of this controller is depicted in Fig. 4.6. Note that the controller provides integral action only for frequencies below $5 \cdot 10^{-5}$ [rad/s]. With the RC-Toolbox, a different controller is computed achieving $\gamma = 0.85$, which might be due to distinct solution procedures in the MATLAB toolboxes. Moreover, the Bode plots for both controllers are different for frequencies below 10^{-4} [rad/s] and above 10^2 [rad/s].

In Fig. 4.7 it is illustrated that the frequency domain specifications are met with controller (4.10). As expected, $|W_y(\mathrm{j}\omega)S(\mathrm{j}\omega)|$ dominates for low frequencies ($\omega < 100$ [rad/s]), while $|W_u(\mathrm{j}\omega)R(\mathrm{j}\omega)|$ dominates for high frequencies ($\omega > 100$ [rad/s]).

Simulation results with controller (4.10) for $w^* = 3.5$ [mm] and $w^* = -3.5$ [mm] (main task) are depicted in Fig. 4.8. The time domain specifications are met, except for a slight overshoot when returning from $x_1 = 3.5$ [mm] to $x_1 = 0$ [mm]. For stepwise changes of magnitude 0.1 [mm] all specifications are met (not depicted).

Unfortunately, for stepwise changes of 6 and 12 [mm] the specifications are *not* met, see Fig. 4.9. From this figure it is concluded, that saturation also occurs for $w^* = \pm 3.5$ [mm] (I), but that it does not cause trouble in this case. A striking phenomenon is, that x_1 does not reach $w^* = -6$ [mm], though the input is well between the saturation bounds (part (II) of the traject). This is probably due to the fact that x_1 is in the low-frequency region for which the controller gain is very small, see Fig. 4.6. Another remarkable result is, that right after part (III) of the traject x_1 does not return to zero. The input u seems unnecessarily large and x_1

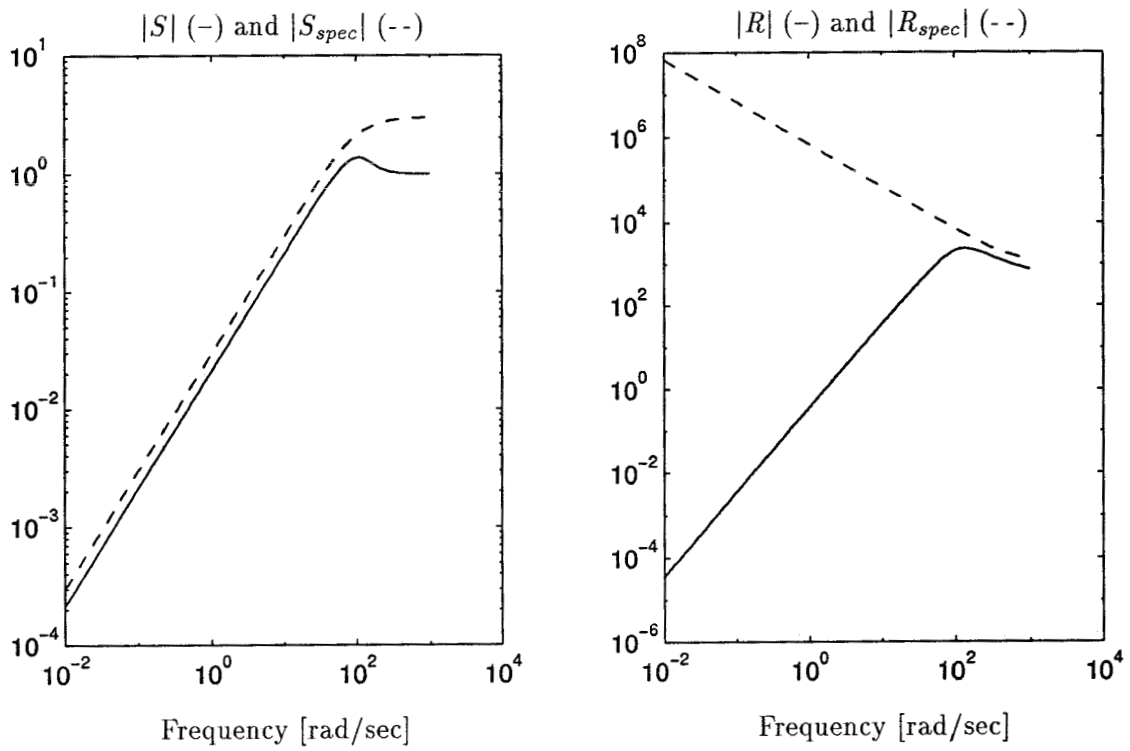

Figure 4.7: Satisfaction of frequency domain specifications

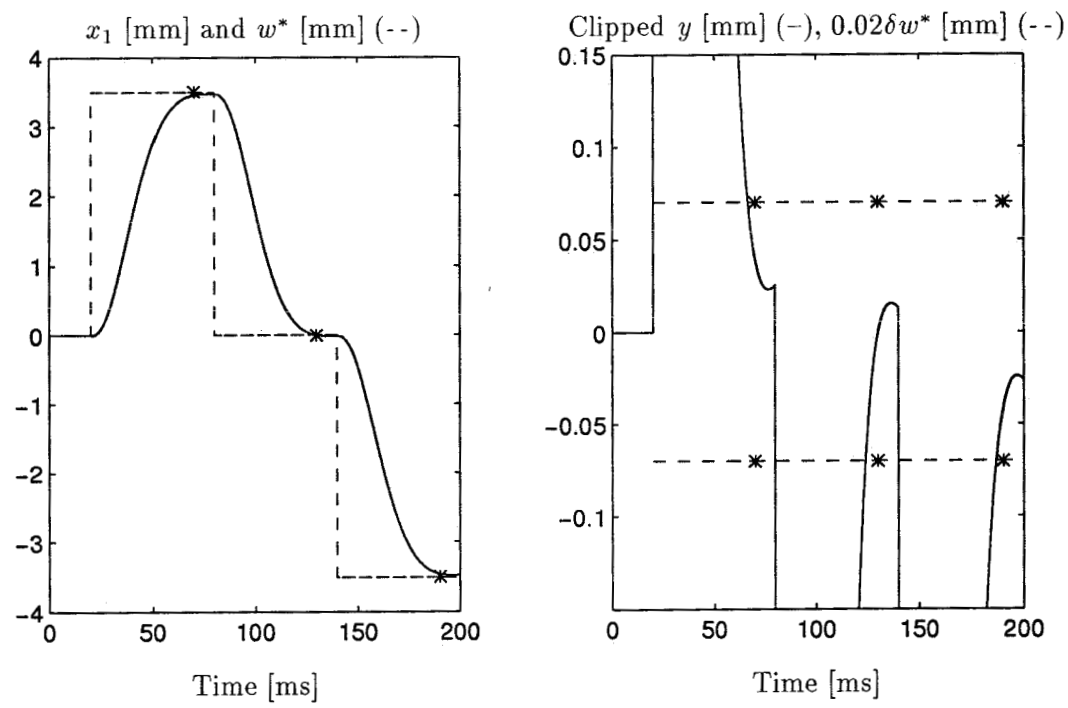

Figure 4.8: Simulation with controller (4.10) for $w^* = \pm 3.5$ [mm]

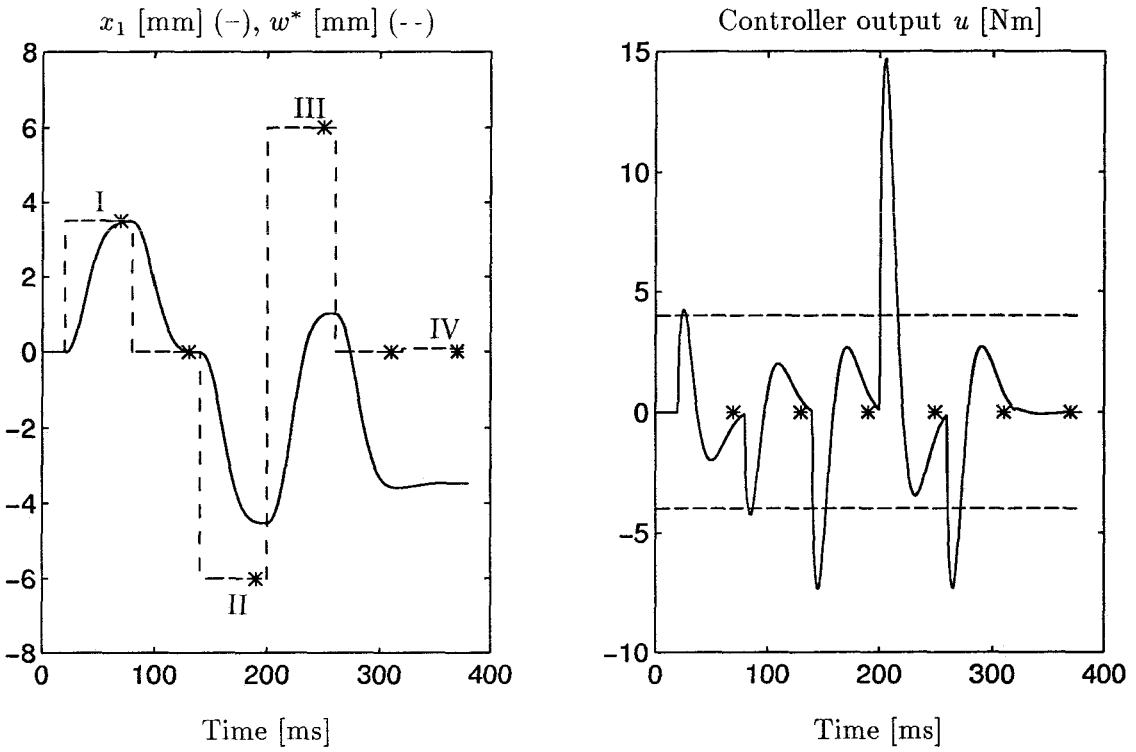

Figure 4.9: Simulation with controller (4.10)

shoots through to -3.6 [mm]. Moreover, for $w^* = 0.1$ (IV) u is almost zero, although x_1 is far from its desired value. Again, the latter phenomenon is due to the fact that the controller provides "integral action" only in the frequency region below $5 \cdot 10^{-5}$ [rad/s].

If it is attempted to improve the response to step-wise changes of 6 [mm] (*e.g.*, by raising ζ in $R_{spec,1}$), the response to smaller step-wise changes deteriorates, in the sense that overshoot occurs.

4.2.2 Saturation as a sector bounded uncertainty

In this section, input saturation will be accounted for in the controller design by modeling the nonlinear saturation element in Fig. 3.1 as a bounded uncertainty, see, *e.g.*, [8, Section 5.5.5] and [2, Chapter 1].

In Fig. 4.10, the saturation element is modeled as the parallel connection of a gain (0.5) and a so-called "sector bounded" uncertainty Δ_u. The perturbation Δ_u is a nonlinear operator that maps the signal u_1 into the signal $v = \Delta_u u_1$. For this mapping holds that $\|\Delta_u u_1\|_2 \leq 0.5\|u_1\|_2$ for every input u_1 to Δ_u. Because of this relation, the perturbation Δ_u is called sector bounded, and has an "∞-norm" which equals 0.5. The basic stability robustness results of Chapter 2 also apply for this type of perturbation.

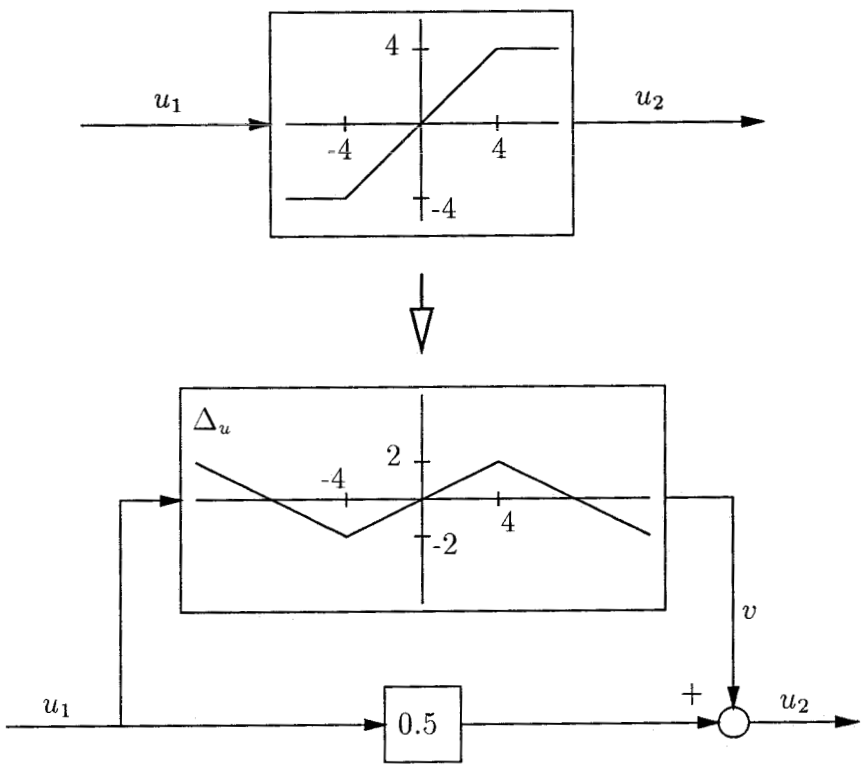

Figure 4.10: Modeling saturation as an additive uncertainty

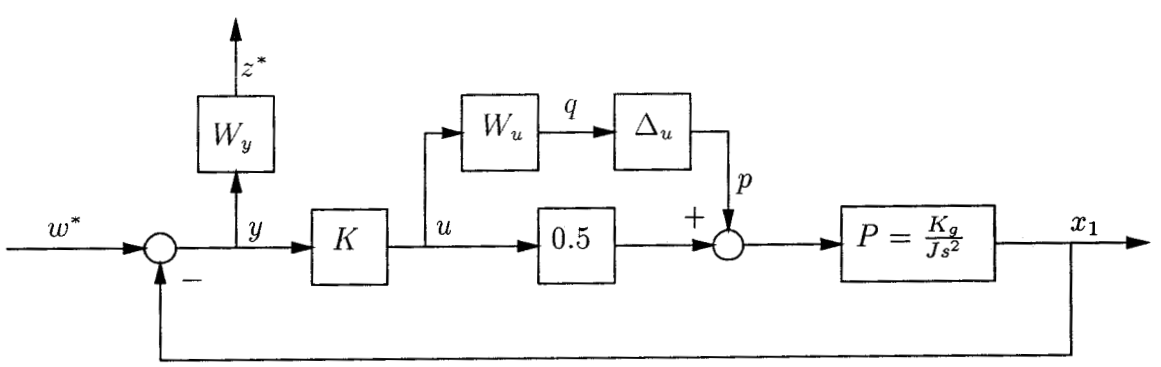

Figure 4.11: Perturbed control system including weighting functions

The control problem formulation is now based on the representation in Fig. 4.11. Comparing this system with Fig. 2.1, it is concluded that $z = [q\ z^*]^T$ and $w = [p\ w^*]^T$. The generalized plant G and the closed-loop TFM M can be written as follows:

$$G = \begin{bmatrix} 0 & 0 & W_u \\ -W_y P & W_y & -0.5 W_y P \\ -P & 1 & -0.5P \end{bmatrix}, \tag{4.11}$$

$$M = \begin{bmatrix} -W_u PK(1+0.5PK)^{-1} & W_u K(1+0.5PK)^{-1} \\ -W_y P(1+0.5PK)^{-1} & W_y(1+0.5PK)^{-1}) \end{bmatrix}. \tag{4.12}$$

The weight $W_u = 0.5$ is chosen so $\|p\|_2 = \|\Delta_u q\|_2 \leq \|q\|_2$. Obviously, this is a *Robust Performance* (RP) control problem with a *structured* 2×2 perturbation block $\Delta = \text{diag}(\Delta_u, \Delta_p)$. Compared with the approach discussed in Section 4.2.1, there is now only one weighting function to be specified. This might be an advantage in an iterative design procedure, since fewer parameters have to be considered. The inverse of $S_{spec,1}$ (4.2) will be used as W_y.

The D-K iteration procedure discussed in Section 2.3 will be applied for μ-synthesis. For this purpose, an initial stabilizing $\mathcal{H}_\infty$ controller will be designed. Since it is expected that fewer iteration steps have to be made if γ for the initial controller is close to 1, κ and a in $S_{spec,1}$ are set accordingly. For the controller design, the μ-Toolbox will be used. With the RC-Toolbox problems occur, as will be indicated.

With $\kappa = 10$ and $a = 150$ an $\mathcal{H}_\infty$ controller is computed that achieves $\gamma = 9.54$. The structured singular values $\mu_\Delta(M)$ for successive controller designs are depicted in Fig. 4.12. For a good fit and a fast convergence, the order of the approximate diagonal scaling D should be high during D-K iteration. However, for implementation reasons the controller order is desirably low, and, consequently, the order of the fit must be low, see Section 2.3. For this reason, the order of the fit to D is fixed at 1 for the first iteration steps (if it is set higher, numerical problems occur during D-K iteration), except for the final iteration, when it is set to 0. So, like the generalized plant, the controller $K(s)$ computed for the third iteration has order 3:

$$K(s) = \frac{9.75 \cdot 10^8 s^2 + 3.81 \cdot 10^{10} s + 7.24 \cdot 10^{11}}{s^3 + 7.95 \cdot 10^4 s^2 + 1.48 \cdot 10^7 s + 6.62 \cdot 10^{-2}}. \tag{4.13}$$

The left plot of Fig. 4.12 shows the magnitude of this controller. Note the large difference between controller (4.13) and controller (4.10), whose magnitude is depicted in Fig. 4.6.

From the right plot in Fig. 4.12, it is concluded that for successive designs $\mu_\Delta(M)$ is flattened over the frequency range of interest. The peak value of $\mu_\Delta(M)$ decreases, while it shifts to higher frequencies. Unfortunately, RP is not guaranteed for controller (4.13), since $\|M\|_\Delta = 2.07$. Continuing the D-K iteration, it seems that $\|M\|_\Delta$ can not be reduced further than about 1.33. Ultimately, $\mu_\Delta(M)$ equals 1 for the whole frequency range, except for a small bump for frequencies above 100 [rad/s]; $\|M\|_\Delta = 1.33$ at $\omega = 1000$ [rad/s]. However, for this continued D-K iteration numerical problems occur, and the resulting controller cannot be relied upon.

As it is clear from Fig. 4.12, for low frequencies the structured singular value is equal to one for all controllers designed during D-K iteration. It appears that this is due to the modeling

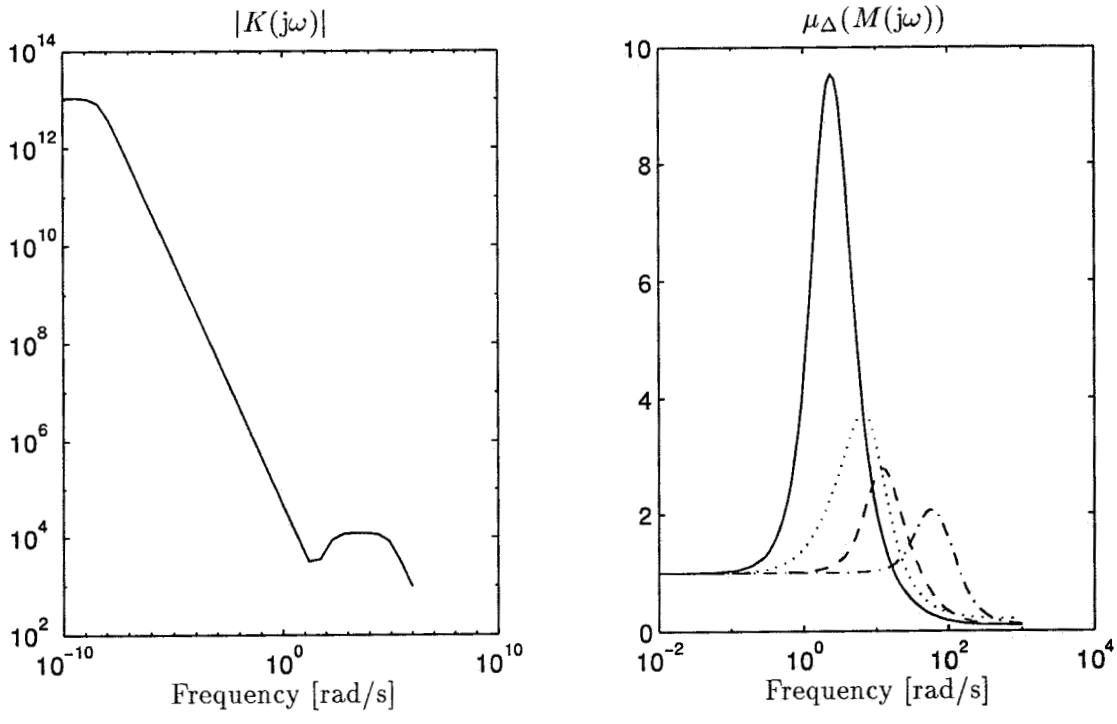

Figure 4.12: *left plot:* magnitude of the final controller $K(s)$ in (4.13); *right plot:* structured singular value of M for four successive designs: initial design (–), first iteration (··), second iteration (- -), third iteration (–·)

of the saturation element: if W_u is set to $\alpha \cdot 0.5$, $\mu_\Delta(M(0))$ equals α. It is also noted, that for the final design $|M_{11}(j\omega)|$ in (4.12) equals one in approximately the same frequency region as $\mu_\Delta(M(j\omega))$ does. For this reason, it seems that $|M_{11}|$ is restrictive for controller design, *i.e.*, $|M_{11}|$ seems to prevent that γ can be made smaller than 1. Suppose that for $s \approx 0$ the controller $K(s)$ is given by $K(s) = \lambda s^k$. Transfer function $M_{11}(s)$ can then be written $\frac{-1}{\zeta s^{(2-k)}+1}$, with $\zeta = \frac{J}{\lambda \cdot 0.5 \cdot K_g}$. So, a controller with $k \geq 2$ yields $|M_{11}(0)| < 1$, otherwise $|M_{11}(0)| = 1$. Apparently, designing a controller with $k \geq 2$ is impossible. On the other hand, if tracking performance is excluded during controller design ($W_y = 0$), the RP problem becomes a RS problem, and M reduces to $M_{11} = -0.5PK(1+PK)^{-1}$ in (4.12). In this case a robustly stabilizing controller $K(s) = 0$ is computed achieving $\gamma \approx 0$. Thus, robust stability (represented by M_{11}) seems to be restrictive *only* in combination with tracking performance.

It is emphasized that a sound explanation for not meeting the frequency domain specifications is lacking at the moment. Anyway, the source of this problem seems to be the suggested way of accounting for saturation, which is probably too conservative, and leads to overly demanding design specifications.

In Fig. 4.13, some simulation results for controller (4.13) are depicted. Obviously, the time domain specifications are not met, not even for small step wise changes. It is remarkable, that for $w^* = \pm 3.5$ [mm] input saturation occurs for a relatively large time interval after a change in w^* (compare with Fig. 4.9).

In case the RC-Toolbox is used for controller design [2, `musyn`], it is noted that the order of the controller does *not* necessarily equal the order of $G(s)$ plus twice the order of D. For instance, if first order diagonal scalings are used, a fifth order K is expected, but higher order controllers might be computed during D-K iteration. The difference with the results obtained with the μ-Toolbox might be due to distinct methods of finding the diagonal 2×2 scaling TFM $D(s) = \text{diag}(d_1(s), d_2(s))$: in the μ-Toolbox, the second diagonal entry $d_2(s)$ is normalized to one, hence need not be fitted, while in the RC-Toolbox both $d_1(s)$ and $d_2(s)$ are fitted.

4.3 Design and evaluation for load disturbance and Coulomb friction

In this section, the control problem is focussed on achieving set-point tracking under load disturbance M_l and under Coulomb friction M_{fr}, see Fig. 3.1. For the purpose of controller design, M_l and M_{fr} have to be incorporated in the standard plant setting of Fig. 2.1. It is emphasized, that controller design *and* evaluation are performed in the *absence* of saturation.

The static load disturbance is represented in the exogenous input w^*, while a "shaping filter" V_1 is added to G to account for the nature of M_l. For a constant disturbance like M_l, this is done by choosing $V_1 = \rho_1 M_l / s$, where ρ_1 is used as a design parameter.

Incorporating the highly nonlinear Coulomb friction in the *linear* standard control problem

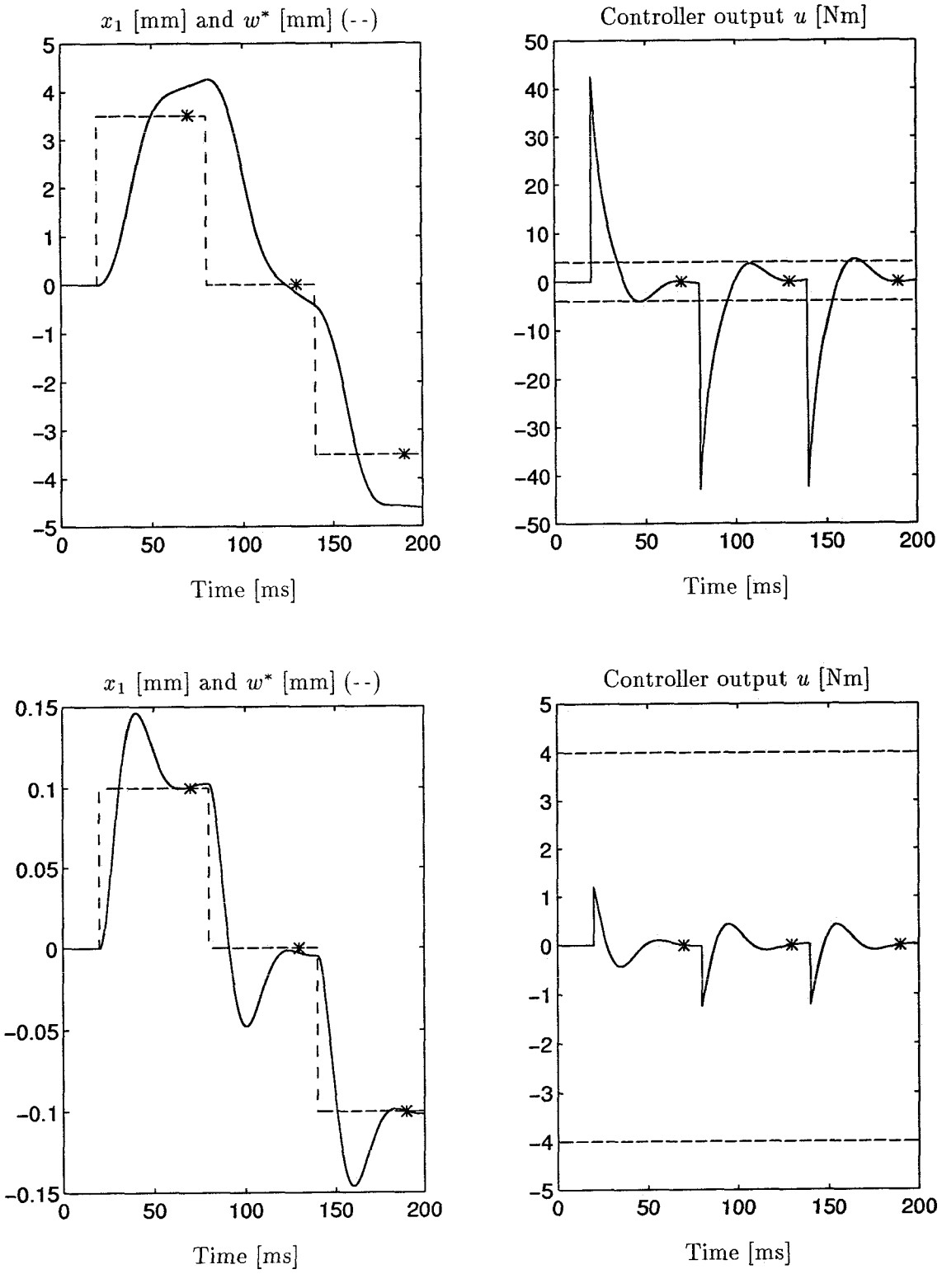

Figure 4.13: Simulations with controller (4.13) for $w^* = \pm 3.5$ [mm] and $w^* = \pm 0.1$ [mm]

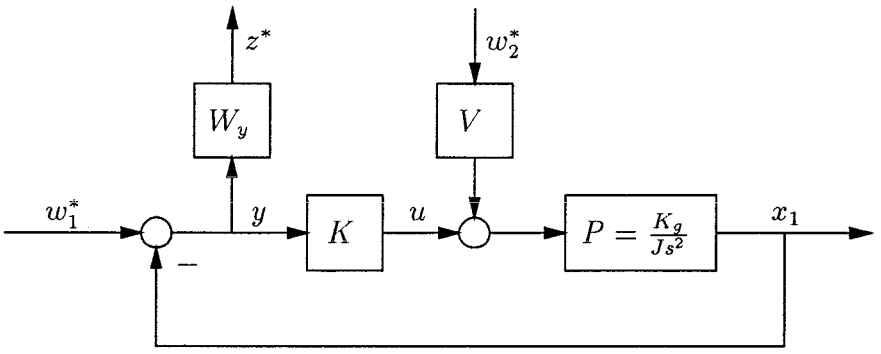

Figure 4.14: Control system including shaping filter for load disturbance and Coulomb friction

set-up is less straightforward. The friction characterization must be linear, possibly accompanied by a bounded perturbation on that linear description. However, in [9] it is shown that this is impossible, which is due to the discontinuity for $x_2 = 0$. For this reason, an alternative "solution" is proposed in [9], which resulted in a successful application for an inverted pendulum. The Coulomb friction is now modeled as an *external* disturbance moment by adding it to w^* and adding a shaping filter V_2 to the plant G. Note that the knowledge of the feedback nature of the friction is lost in this way. Only *where* the friction moment acts on the system is emphasized. In order to account for both slip ("step") and stick ("impulse"), V_2 is chosen as follows:

$$V_2 = \rho_2 \frac{M_c}{s} \text{ (slip)} + \rho_3 M_h \text{ (stick)} = \frac{\rho_2 M_c + \rho_3 M_h s}{s}. \tag{4.14}$$

Shaping filters V_1 and V_2 are now added up, so shaping filter V in Fig. 4.14 is described as follows:

$$V = \frac{\rho_1 M_l + \rho_2 M_c + \rho_3 M_h s}{s}. \tag{4.15}$$

For the control system in Fig. 4.14, the generalized plant G and closed-loop system M are given by the following relations:

$$G = \begin{bmatrix} W_y & -W_y PV & -W_y P \\ 1 & -PV & -P \end{bmatrix}, \quad M = \begin{bmatrix} W_y S & -W_y PSV \end{bmatrix}. \tag{4.16}$$

Again, this is a NP control problem with a 2×1 unstructured fictitious perturbation block Δ_p. In order to meet the rank condition on D_{12}, a small weight on u is added ($W_u = 10^{-8}$). Before it is attempted to design a controller achieving $\|M\|_\infty < 1$, it is emphasized that controller (4.3) does *not* achieve the time domain specifications under load disturbance and Coulomb friction, which indicates the need to account for these phenomena.

During controller design $W_y = S_{spec,1}^{-1}$ in (4.2) will be used with $\kappa = 2$ and $a = 100$, see Table 4.3. Finding the "best" settings for the design parameters in V is again an arduous trial-and-error procedure. To start with, ρ_1, ρ_2, and ρ_3 are set to guarantee a fast rejection of M_l, while limiting the displacement x_1. It is noted, that $\|M\|_\infty < 1$ is easier achieved and

$S_{spec,1}$	V
$\kappa = 2$	$M_l = 1.5$
$a = 100$	$M_c = 0.8$
	$M_h = 3 \cdot M_c$
	$\rho_1 = 10^7$
	$\rho_2 = 10^7$
	$\rho_3 = 0$

Table 4.3: Parameters for sensitivity specification $S_{spec,1}$ and shaping filter V

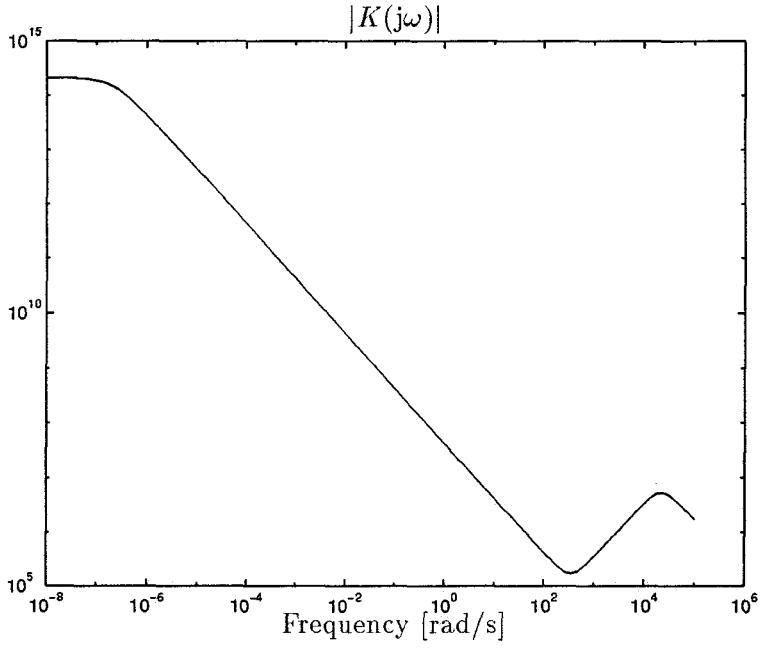

Figure 4.15: Magnitude plot of controller (4.18)

better disturbance rejection is obtained if V is replaced by $V^* = VW_y^{-1} = VS_{spec,1}$. With this modification, the closed-loop system M in (4.16) reduces to:

$$M = \begin{bmatrix} W_y S & -PSV^* \end{bmatrix}. \tag{4.17}$$

An additional advantage of this modification is, that weighing PS (influence of w_2^* on z^*) can now be performed independently of the weight on S (influence of w_1^* on z^*).

Studying various simulations, the "best" compromise between tracking on the one hand and rejection of Coulomb friction and load disturbance on the other hand, seems to be achieved with the settings in Table 4.3. Note that ρ_3 is fixed at zero, since it is observed that a non-zero ρ_3 does not improve performance. With the μ-Toolbox the following controller achieving $\gamma = 0.56$ is computed:

$$K(s) = \frac{1.73 \cdot 10^{11} s^3 + 1.03 \cdot 10^{14} s^2 + 2.97 \cdot 10^{16} s + 2.12 \cdot 10^{18}}{s^4 + 3.22 \cdot 10^4 s^3 + 4.96 \cdot 10^8 s^2 + 4.92 \cdot 10^{10} s + 9.91 \cdot 10^3}. \tag{4.18}$$

The magnitude of this controller is depicted in Fig. 4.15.

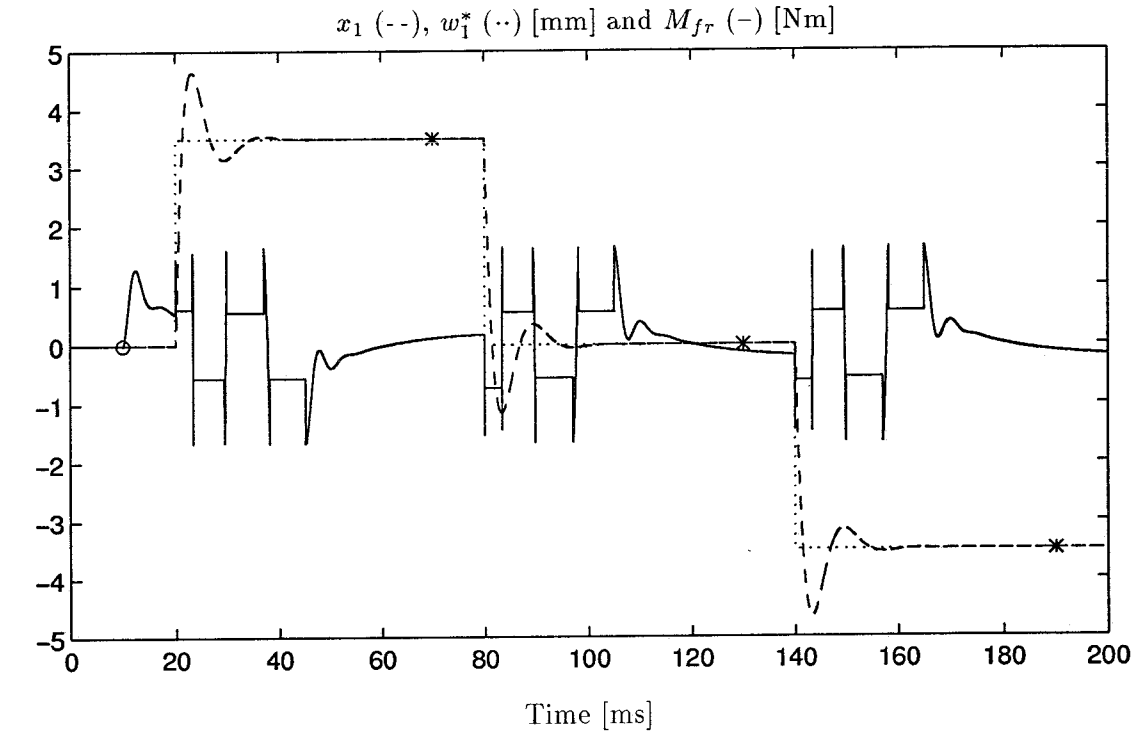

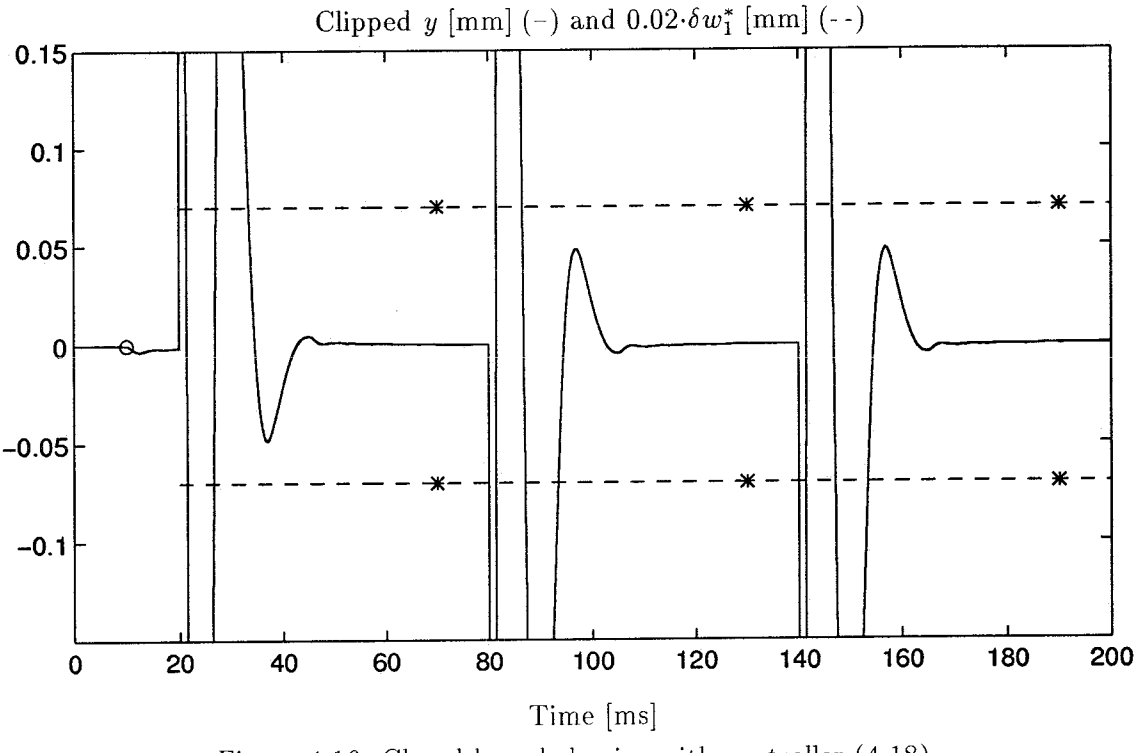

Figure 4.16: Closed-loop behavior with controller (4.18)

Figure 4.16 shows some results of a simulation with (4.18), for which the following friction parameters are used (see Section 3.2): $p_0 = 0.1 \cdot 2\pi \cdot 0.04/K_g$, $M_c = 0.55$, $\lambda = M_c/p0$, $\psi = 2$ ($M_h = 3M_c$), $\beta = 0$ (it is observed that if $\beta \neq 0$ the Coulomb friction model does not always work correctly, in the sense that the maximum stick friction might be larger than the slip friction even if $\psi = 0$). The symbol "o" in Fig. 4.16 indicates the time at which M_l starts to act on the system.

Obviously, the third time domain specification is not met, since overshoot occurs. Note that the influence of M_l on the tracking error is only marginal. The same applies for the influence of M_{fr}: if the response in Fig. 4.16 is compared with the one resulting from a simulation without Coulomb friction, it is concluded that these responses are approximately the same. Apparently, rejection of load disturbance and Coulomb friction is more restrictive for controller design than tracking specifications, *i.e.*, $|-PSV^*|$ dominates over $|W_yS|$. In order to avoid overshoot, M_{11} (tracking) must be emphasized during controller design. Unfortunately, a controller with only one input y which leads to better performance than the one in (4.18) has not been found.

4.4 Multi-input controllers

In this section, it is attempted to obtain better performance by designing controllers with 2 and 3 inputs respectively. Firstly, a controller with 2 inputs as depicted in Fig. 4.17 will be studied. While the input for the previously studied controller was the *difference* between the desired position and the real position, *i.e.*, the tracking error, a controller will now be studied which uses the desired position w_1^* and the real position x_1 as two *independent* inputs. The generalized plant for Fig. 4.17 is described as follows:

$$G = \begin{bmatrix} W_y & -W_yPV & -W_yP \\ 1 & 0 & 0 \\ 0 & PV & P \end{bmatrix}. \tag{4.19}$$

In order to make D_{12} full column rank, a very small weight is imposed on u. In addition, a very small "measurement error" on x_1 is used to have D_{21} full row rank. With the parameters for $S_{spec,1}$ and V as in Table 4.4, an $\mathcal{H}_\infty$ controller is designed with the μ-Toolbox achieving $\gamma = 0.51$. It is remarked that a controller obtained with the parameters in Table 4.3 meets the frequency domain specifications (*and* the time domain specifications) as well. However, this design leads to unnecessarily large controller gains, which can be circumvented by reducing ρ_1 and ρ_2. In Fig. 4.18, the frequency-dependent singular value of the computed 1×2 controller $K(s)$ is depicted.

With this controller the time domain specifications are (easily) achieved, see Fig. 4.19. The Coulomb friction parameters are the same as in the previous section. If M_c is raised to 0.8, maintaining $M_h = 3 \cdot M_c$, the specifications are still met. Moreover, the influence of the static load disturbance and the Coulomb friction appears to be neglectable, since a simulation with $M_l = M_{fr} = 0$ shows approximately the same tracking error behavior as in Fig. 4.19.

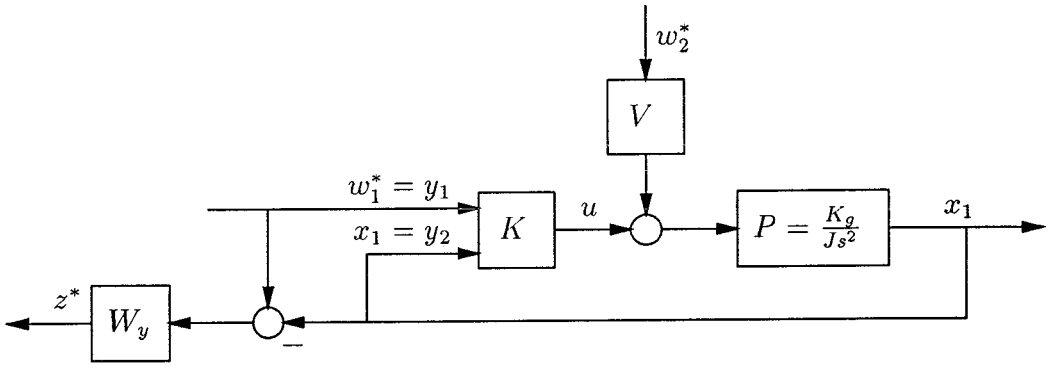

Figure 4.17: Controller with two inputs y_1 and y_2

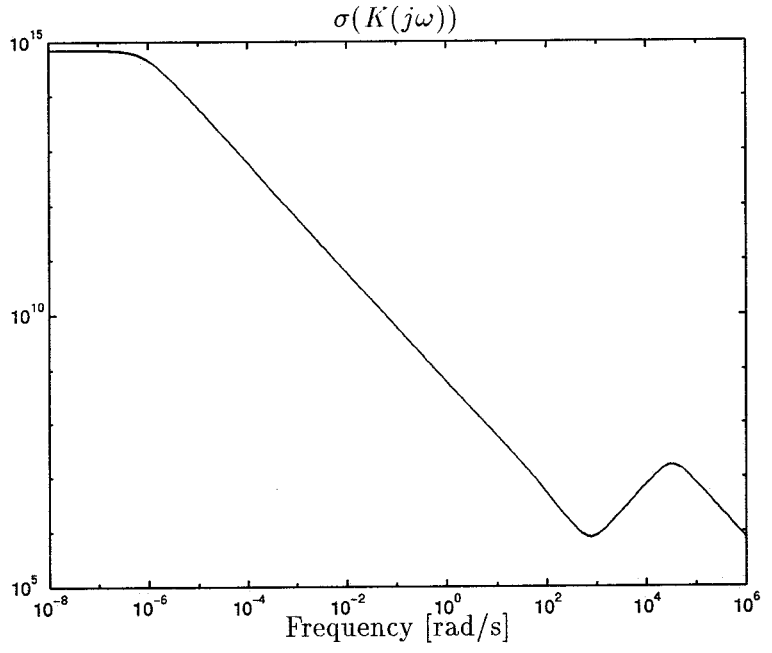

Figure 4.18: Singular value of the controller with two inputs y_1 and y_2

$S_{spec,1}$	V
$\kappa = 2$	$M_l = 1.5$
$a = 100$	$M_c = 0.8$
	$M_h = 3 \cdot M_c$
	$\rho_1 = 1$
	$\rho_2 = 1$
	$\rho_3 = 0$

Table 4.4: Parameters for sensitivity specification $S_{spec,1}$ and shaping filter V

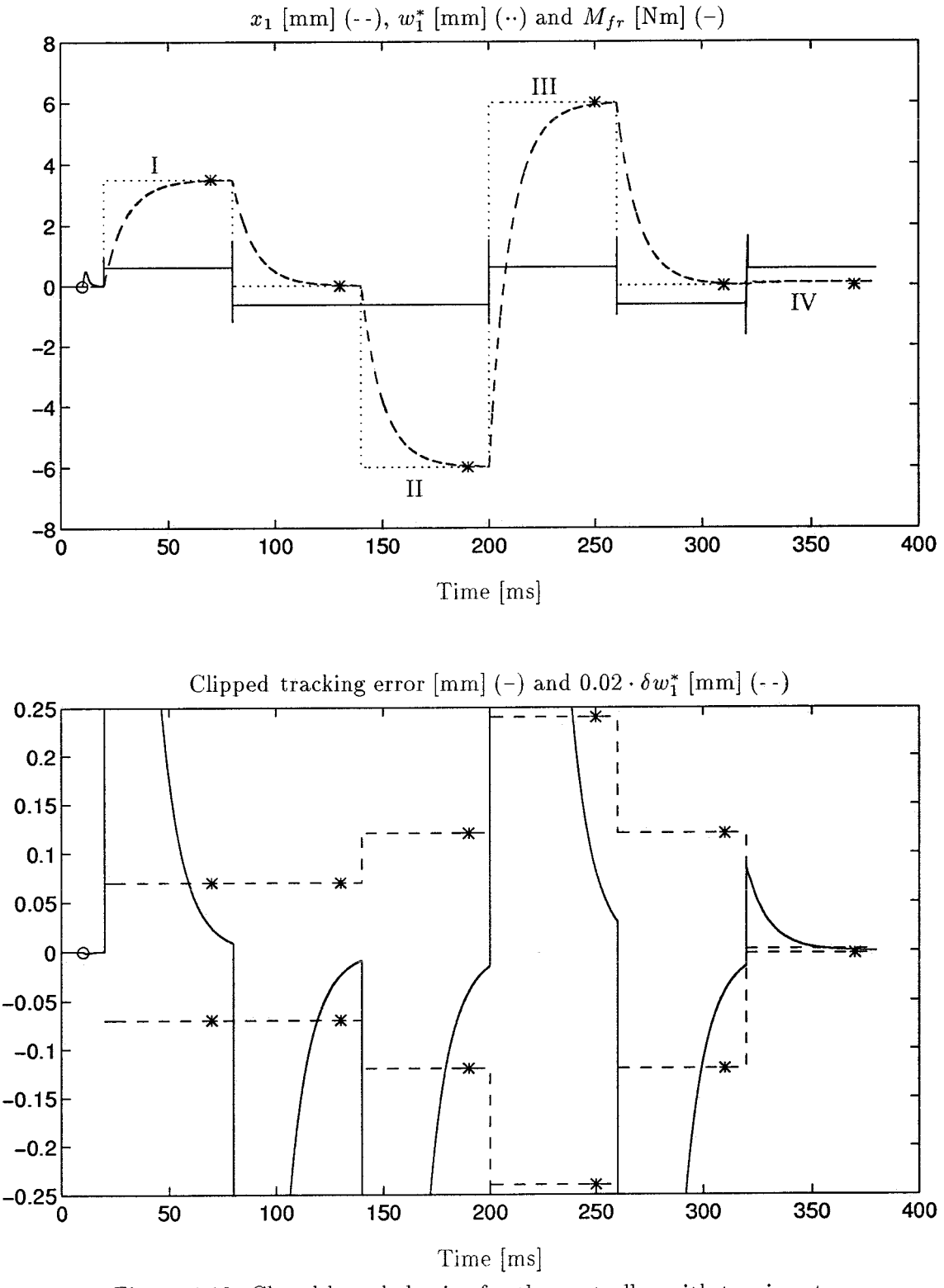

Figure 4.19: Closed-loop behavior for the controller with two inputs

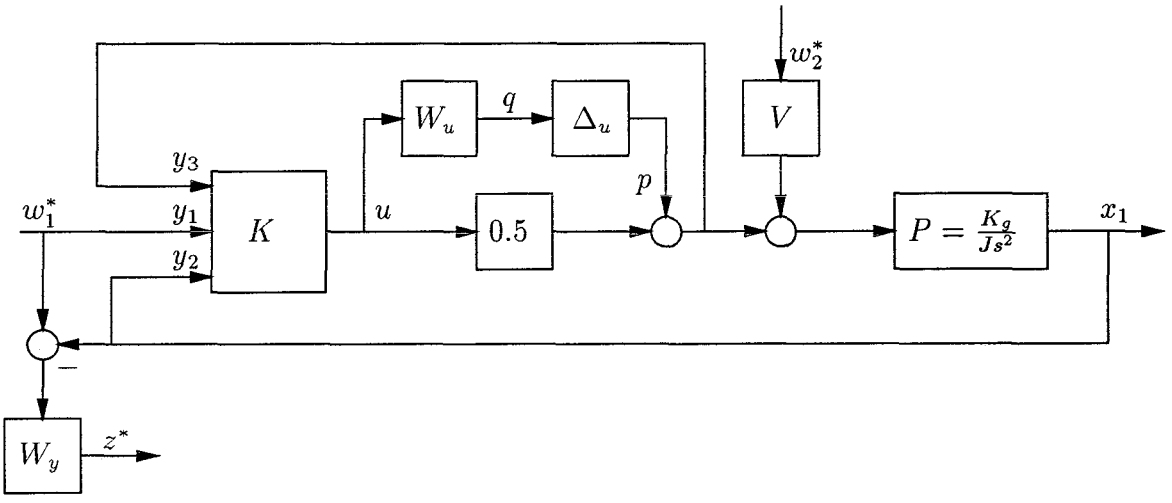

Figure 4.20: Controller with three inputs y_1, y_2 and y_3

Note, that this result is obtained in the *absence* of controller output saturation. If the simulation model is extended with the saturation element, and saturation is accounted for by weighing the controller output, as it is done in Section 4.2.1, a two-input controller design is not successful. A good response was only achieved for $w_1^* = \pm 0.1$ [mm]. Therefore, a final attempt to design for saturation is made by modeling the saturation element as a sector bounded uncertainty, see Section 4.2.2. For this purpose, a controller with three inputs as depicted in Fig. 4.20 will be designed by μ-synthesis.

Three signals are fed back to the controller $K(s)$: the desired position w_1^*, the real position x_1, and the output of the saturation block, *i.e.*, the applied input. Comparing Fig. 4.20 with Fig. 2.1, it is concluded that this is a RP control problem with $z = [q\ z^*]$, $w = [p\ w_1^*\ w_2^*]$, and with a *structured* perturbation block Δ consisting of a 1×1 block Δ_u and a 3×1 block Δ_p. The generalized plant G is given by:

$$G = \begin{bmatrix} 0 & 0 & 0 & W_u \\ -W_y P & W_y & -W_y PV & -0.5 W_y P \\ 0 & 1 & 0 & 0 \\ P & 0 & PV & 0.5P \\ 1 & 0 & 0 & 0.5 \end{bmatrix}. \tag{4.20}$$

Designing a controller with the parameters in Table 4.4, a fourth order controller is designed by μ-synthesis. After two iterations, $\mu_\Delta(M)$ is flat for the whole frequency range of interest, and equals one. As in Section 4.2.2, the μ-value depends on the value of W_u. A sound explanation for this phenomenon has not been found. Although the frequency domain requirements are not met ($\|M\|_\Delta = 1$), a simulation with the computed controller is performed. It is concluded that the closed-loop behavior is only satisfactory for $w_1^* = \pm 0.1$ [mm]. For $w_1^* = \pm 3.5$ [mm] or $w_1^* = \pm 6$ [mm], all time domain requirements are violated, which is due to input saturation.

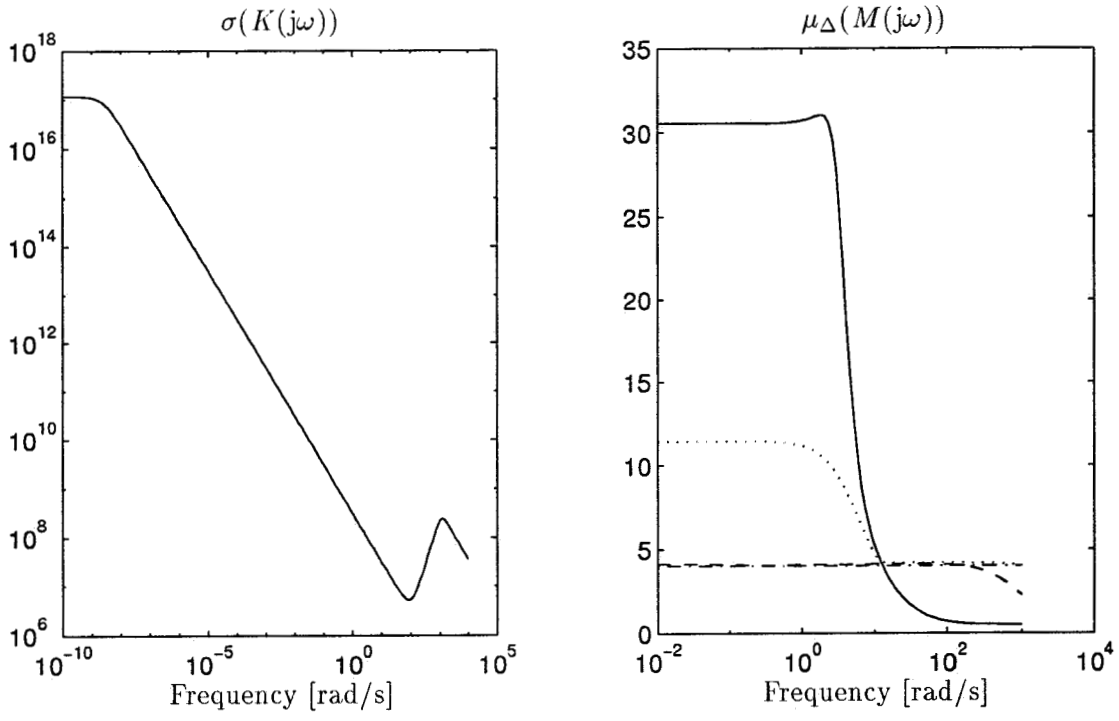

Figure 4.21: *left plot:* singular value of the controller with three inputs y_1, y_2 and y_3; *right plot:* structured singular value of M for four successive designs: initial design (–), first iteration (··), second iteration (- -), third iteration (–·)

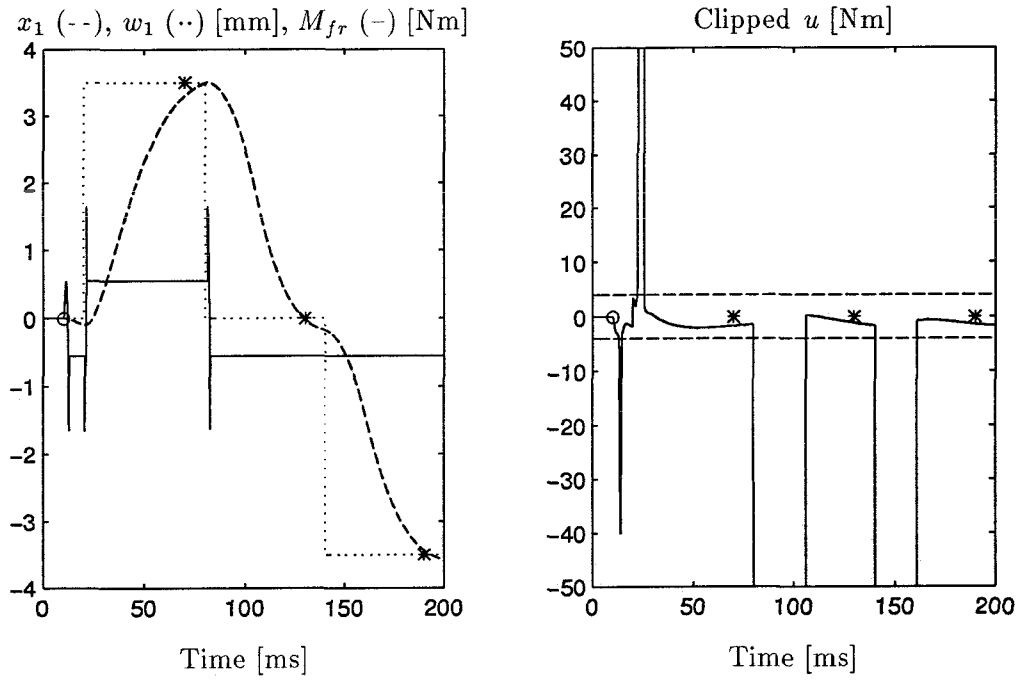

Figure 4.22: Closed-loop behavior for $w_1^* = \pm 3.5$ [mm] for the controller with three inputs

It is attempted to make the design more "robust" to saturation by raising W_u to 2 and maintaining the parameters in Table 4.4. A 1×3 controller achieving $\mu_\Delta(M(j\omega)) = 4$ is now computed, the frequency-dependent singular value of which is depicted in the left plot of Fig. 4.21. The structured singular value of M for successive controller designs is depicted in the right plot. The response for the main task ($w_1^* = \pm 3.5$ [mm]) indeed improves, see Fig. 4.22, although the specifications are not met. In fact, this behavior is the best which has been found for a number of designs in which both W_u and the parameters in V and $S_{spec,1}$ were changed iteratively. Note, that the controller output still saturates for a large time interval after a stepwise change in w_1^*. For $w_1^* = \pm 0.1$ [mm] or $w_1^* = \pm 6$ [mm], the response is somewhat worse.

Chapter 5

Conclusions and recommendations

In this report, $\mathcal{H}_\infty$- and μ-based controller design methods were studied. The main findings with these approaches are discussed in Section 5.1. Conclusions and recommendations with respect to the electro-mechanical actuator control problem are in Section 5.2.

5.1 $\mathcal{H}_\infty$-optimization and μ-synthesis

Performance specifications for control systems are often formulated in the time domain. Contrary to the case of frequency domain specifications, it might then be difficult to find suitable weighting functions for controller design, since it is not always trivial to translate time domain specifications into frequency domain equivalents. Moreover, meeting the frequency domain specifications does not imply that the time domain specifications are met as well. Conversely, if the frequency domain specifications are *not* met, the time domain specifications might still be met. In case of frequency domain requirements, *e.g.*, for a pure disturbance attenuation problem, the choice of weighting functions is rather straightforward. In order to avoid high-order controllers, low-order weighting functions are advisable.

The algorithms for controller design in both the RC-Toolbox and the μ-Toolbox require the generalized plant $G(s)$ to be proper. This puts restrictions on the type of weighting functions to be used, since they must be chosen to meet this requirement. For example, a non-proper output-disturbance weight (specifying roll-off for high frequencies) might cause $G(s)$ to be non-proper (in [8, Section 6.7] it is explained how this particular problem can be circumvented).

In order to design controllers with the MATLAB toolboxes, the standard assumptions in Section 2.2 need to be satisfied. In the first place, the rank conditions on D_{12} and D_{21} are not always satisfied. To "solve" this shortcoming, it might be necessary to introduce artificial control objectives in z and artificial external inputs in w. Due to this modification, controller design becomes sub-optimal. Conservativeness of the controller must be limited by imposing

very low weights on the artificial signals. Another frequently encountered problem is due to eigenvalues of G on the imaginary axis (see Section 4.1), by which fulfillment of the third and fourth standard assumption is endangered. This problem can be solved by a bilinear transformation on the generalized plant, by which the eigenvalues are shifted, followed by standard controller design. This modification results in a sub-optimal controller, which is not always a problem.

Performing μ-synthesis with one of the MATLAB toolboxes is sometimes troublesome. Firstly, the μ-value may increase for successive designs in D-K iteration. Secondly, numerical problems in solving the associated Riccati equations might occur during $\mathcal{H}_\infty$ controller design for the scaled system (fourth step in D-K iteration). Moreover, a satisfactory fit to D is not always possible due to numerical conditioning problems of the D scales, and a lower order fit must be used (third step of D-K iteration). In this report, the controller order was restricted by using a zero order fit in the final iteration, provided that the μ-value did not increase. An alternative is to apply order reduction to the final design, see, *e.g.*, [8, Section 6.10.7]. If the RC-Toolbox is used, it is noted that the order of the controller is not always equal to the order of $G(s)$ plus twice the order of $D(s)$. The reason for this is unclear.

5.2 Controller design for the electro-mechanical actuator

Designing a controller which meets the time domain specifications appeared to be infeasible. Only for the system without saturation, satisfactory performance was achieved. Moreover, design for tracking, load disturbance and Coulomb friction was only successful for a controller which uses the desired position and the measured one as two *individual* input signals. In case the difference between those signals (the tracking error) is fed back to the controller, the time domain specifications were *only* met in the absence of saturation, load disturbance, and Coulomb friction. Again, it is emphasized that the choice of the type and the parameters of the weighting functions and the shaping functions was not straightforward; modifying parameters or applying different types of weights might result in significant differences in closed-loop behavior.

In order to account for input saturation, the nonlinear saturation element was modeled as a sector bounded uncertainty. Unfortunately, μ-synthesis was not successful, since the requirements in both the time domain *and* the frequency domain were violated. The μ-value appeared to depend on the conic sector parameter W_u. A sound explanation for this phenomenon is currently lacking and needs further attention.

For the purpose of controller design the Coulomb friction was modeled as an external input disturbance. In the absence of saturation, this approach proved to be successful. Nevertheless, a recommendation is to search for a way to incorporate Coulomb friction in the linear control system set-up which accounts for its feedback nature.

In the original control problem formulation in [7], the controller to be implemented should be a digital one, making use of a quantized measurement. However, since the specifications

could not even be achieved with a continuous controller making use of exact measurements, no attention has been paid to this aspect. Only if the problem is solved for the continuous implementation, studying the effects of a digital controller seems worthwhile. For the same reason, accounting for additional modeling errors as mentioned in Section 3.1 is not useful at the moment.

Bibliography

[1] Gary J. Balas, John C. Doyle, Keith Glover, Andy Packard, and Roy Smith, *μ-Analysis and synthesis toolbox*, user's guide, The MathWorks, Natick, MA, USA, 1991

[2] Richard Y. Chiang and Michael G. Safonov, *Robust control toolbox for use with* MATLAB, user's guide, The MathWorks, Natick, MA, USA, 1992

[3] John C. Doyle, Analysis of feedback systems with structured uncertainties, *IEE Proc.*, part D 129, pp. 242-250, 1982

[4] John C. Doyle, Bruce A. Francis and Allen R. Tannenbaum, *Feedback control theory*, MacMillan, London, 1992

[5] D.A. Haessig, Jr. and B. Friedland, On the modeling and simulation of friction, *J. Dynamic Systems, Measurement, and Control*, vol 113, pp. 354-362, Sept. 1991

[6] Bram de Jager, *Practical evaluation of robust control for a class of nonlinear mechanical systems*, PhD thesis, Eindhoven University of Technology, Nov. 1992

[7] H. Kiendl and J.J. Rüger, Elektromechanisches Stellsystem, in *Nichtlineare Regelung: Methoden, Werkzeugen, Anwendungen*, vol. 1026 of *VDI Berichte*, pp. 109-111, Düsseldorf: VDI-Verlag, 1993

[8] Huibert Kwakernaak and Okko H. Bosgra, *Design methods for control systems*, course for the Dutch Graduate Network on Systems and Control, spring term 1993-1994

[9] Gert-Wim van der Linden and Paul F. Lambrechts, $\mathcal{H}_\infty$ control of an experimental inverted pendulum with dry friction, *IEEE Control Systems Mag.*, vol. 13, pp. 44-50, Aug. 1993

[10] Maarten Steinbuch, Pepijn Wortelboer, Pieter J.M. van Groos, Okko H. Bosgra, Limits of implementation: A CD player control case study, in *Proc. of the American Control Conference*, vol. 3, pp. 3209-3213, Baltimore, Maryland, June 1994